



**Western Michigan University
ScholarWorks at WMU**

Master's Theses

Graduate College

4-1-2013

EEG Acquisition System on Mobile Platform

Veerendra Dasari

Western Michigan University, veerendradasari@yahoo.com

Follow this and additional works at: http://scholarworks.wmich.edu/masters_theses

Recommended Citation

Dasari, Veerendra, "EEG Acquisition System on Mobile Platform" (2013). *Master's Theses*. Paper 118.

This Masters Thesis-Open Access is brought to you for free and open access by the Graduate College at ScholarWorks at WMU. It has been accepted for inclusion in Master's Theses by an authorized administrator of ScholarWorks at WMU. For more information, please contact maira.bundza@wmich.edu.



EEG ACQUISITION SYSTEM ON MOBILE PLATFORM

by

Veerendra Dasari

A Thesis submitted to the Graduate College
in partial fulfillment of the requirements
for the Degree of Master of Science in Engineering (Electrical)
Department of Electrical and Computer Engineering
Western Michigan University
April 2013

Thesis Committee:

Dr. Ikhlas Abdel Qader, Ph.D., Chair
Dr. Janos L. Grantner, Ph.D.
Dr. Muralidhar Ghantasala, Ph.D.

EEG ACQUISITION SYSTEM ON MOBILE PLATFORM

Veerendra Dasari, M.S.E.

Western Michigan University, 2013

The Electro-encephalogram [EEG] recording systems play a major role in the Brain Computer Interface machines where the brainwave signals are given as controls. There is a considerable development in transmission of these signals onto different platforms based on the necessity and portability of applications. With the advent of wireless signal transmission protocols for the medical devices, there is an increased research in the domain of offsite patient monitoring applications.

This document describes the evolution prototype of the portable EEG acquisition system developed to acquire the human scalp signals via electrodes and display them on the Android mobile phone after pre-conditioning the raw EEG signals.

An analog circuit was developed to amplify the low amplitude brainwave scalp signals using the instrumentation amplifier and a band pass filter to eliminate the unwanted frequencies due to the surrounding noise sources. A microcontroller digital circuit was implemented to digitize the analog signals and transmit them onto the mobile using the Bluetooth module coupled to the microcontroller. An application was developed on the android platform to display the acquired signals. This prototype is validated by acquiring the EEG signals from a recruited subject by following the guidelines from HSIRB committee at WMU.

Copyright by
Veerendra Dasari
2013

ACKNOWLEDGMENTS

I would like to express my gratitude, appreciation and thanks to my advisor Dr. Ikhlas Abdel Qader for her encouragement and guidance in completion of this thesis. Her guidance helped me to choose a right path to become a successful engineer. I would also like to convey thanks to the members of my thesis committee Dr. Janos Grantner (Professor and Interim Chair, ECE Dept.) and Dr. Muralidhar Ghantasala (Professor, MAE Dept.) for extending their support and time to my thesis.

Electrical and Computer Engineering (ECE) department professors and staff deserve thanks for their support to my thesis. In particular, I would like to thank Dr. Damon Miller and Mr. David Florida for their support in providing the equipment needed for testing and measurement. I would like to thank my fellow lab members Abdoulaye Ousseini, David Anderson, Angie Massiel Paula Sanchez for their support in Digital Signal and Image Processing Lab. Also I would like to thank my friend Raviteja Gadipudi for his support and clearing my doubts in Android Software Development.

Finally, I owe my deepest gratitude and special thanks to my parents, family and friends for their moral support in achieving and reaching to this point of my life.

Veerendra Dasari

TABLE OF CONTENTS

ACKNOWLEDGMENTS	ii
LIST OF TABLES	vi
LIST OF FIGURES	vii
CHAPTER	
I. INTRODUCTION	1
II. PERTINENT LITERATURE AND BACKGROUND	4
2.1. Bioelectric Potentials	4
2.2. Electroencephalography.....	6
2.3. Medical Instrumentation System	8
2.4. Bio-Potential Electrodes	9
2.5. Bio-Potential Amplifiers.....	12
2.6. Analog Bio-Potential Signal Processing	13
2.7. Digital Bio-Potential Signal Processing.....	16
2.8. EEG Acquisition Practices.....	17
2.9. Smart Acquisition Systems	19
2.10. Summary	20
III. SYSTEM DESIGN – HARDWARE AND SOFTWARE.....	21
3.1. Introduction.....	21
3.2. EEG Signal Acquisition.....	22

Table of Contents—continued

CHAPTER

3.3. Amplifier Design	23
3.4. Active Filter Design.....	25
3.4.1. Low Pass Butterworth Filter	27
3.4.2. High Pass Butterworth Filter	32
3.4.3. Notch Filter	36
3.4.4. DC Bias Filter	38
3.5. Power Management	39
3.6. Digital Conversion and Data Transfer Design.....	40
3.6.1. The Microcontroller – MSP430BT5190.....	42
3.6.1.1. Analog to Digital Conversion	42
3.6.1.2. UART mode Transmission	43
3.6.2. CC2560 Bluetooth Operation	45
3.7. Android Application	47
3.8. Summary	49
IV. SYSTEM'S REALIZATION, PARAMETERS AND RESULTS	50
4.1. Analog Circuit Realization on a PCB	50
4.2. Gain and Frequency Response of the Analog Circuitry	52
4.2.1. Amplifier.....	53
4.2.2. Low Pass Filter	54
4.2.3. High Pass Filter.....	55
4.2.4. 60Hz Notch Filter	57

Table of Contents—continued

CHAPTER

4.2.5. DC Bias Filter	58
4.2.6. Frequency Response of Analog Filter Circuit	59
4.2.7. Comparison between Design and Implementations.....	61
4.3. Digital Circuit Realization on MSP-EXP430F5438 CC2560 Evaluation Platform	63
4.3.1. Hardware Connections.....	63
4.3.2. Software Development.....	66
4.3.2.1. Analog to Digital Conversion	67
4.3.2.2. UART Interface (Universal Serial Communication)	69
4.3.2.3. Bluetooth Operation.....	71
4.4. Android Software Implementation	75
4.5. Implementation of Designed EEG Acquisition System.....	78
4.6. Summary	80
V. CONCLUSIONS AND FUTURE SCOPE.....	81
5.1. Conclusions.....	81
4.5. Recommendations for Future Work.....	82
APPENDIX	
HSIRB Approval Letter (Proj. No.: 11-11-12)	83
BIBLIOGRAPHY.....	85

LIST OF TABLES

2.1. Significance of Anatomical Regions of Brain as Shown in Figure 2.2	7
2.2. Types of Brainwaves.....	8
2.3. Types of Surface Recording Electrodes.....	11
3.1. Low Pass Butterworth Filter Specifications	31
3.2. High Pass Butterworth Filter Specifications.....	34
4.1. PCB Design Constraints for Analog Circuit.....	50
4.2. Parameter Matching between the Designed and Implemented Circuits	62
4.3. ADC_12 Register Initialization for 12-bit Analog to Digital Conversion....	67
4.4. USCI Register and Port Initialization for UART Transmission	70

LIST OF FIGURES

1.1.	General EEG Acquisition System.....	2
2.1.	Recording and Interpretation of Action Potential of Cell Membrane.....	5
2.2.	Anatomical Structure of Brain	6
2.3.	Generalized Medical Instrumentation System	9
2.4.	Ion Exchange at Electrode Electrolyte Interface	10
2.5.	Op-Amp Equivalent Circuit.....	13
2.6.	Inverting and Non-Inverting Amplifiers.....	14
2.7.	Active Frequency Filter Models	15
2.8.	Frequency Response of Low Pass and High Pass Filters	15
2.9.	Microcomputers in Signal Processing	17
2.10.	Evolution of EEG Recording Systems.....	18
3.1.	Block Diagram of EEG Acquisition System	21
3.2.	Ag-AgCl Electrodes (Flat and Ear clip) used for EEG Acquisition	22
3.3.	Schematic of the INA128 Instrumentation Amplifier Circuit	24
3.4.	Block Diagram of Active Filter in the Analog Front End Design	26
3.5.	Second Order Unity Gain Sallen-Key Topology	27
3.6.	Sallen-Key Topology of Unity Gain Low Pass Filter.....	28
3.7.	Designed 6 th Order Low Pass Butterworth Filter.....	30
3.8.	Simulated Frequency Response of Designed Low Pass Filter on Pspice	32
3.9.	Sallen-Key Topology of Unity Gain High Pass Filter	33

List of Figures—continued

3.10. Designed 2 nd Order High Pass Butterworth Filter	35
3.11. Simulated Frequency Response of Designed High Pass Filter on Pspice	35
3.12. Twin-T Filter Topology for Notch Filter Design.....	36
3.13. Schematic Diagram of Designed 60Hz Notch Filter	37
3.14. Simulated Frequency Response of Designed Notch Filter on Pspice.....	37
3.15. Schematic Diagram of Designed DC Bias Filter	38
3.16. $\pm 5V$ Voltage Regulator Circuit to Power the Analog Circuit.....	39
3.17. Block Diagram of System's Digital Data Conversion and Data Transfer.....	41
3.18. Hardware Connections for UART Transmission between MSP430BT5190 and CC2560	44
3.19. Block Diagram of CC2560 Chip.....	45
3.20. EtherMind Bluetooth Serial Port Profile Stack Layer	46
3.21. Flowchart for Data Reception using Bluetooth on Android Mobile.....	48
4.1. PCB Layout Design of Analog Circuit	51
4.2. Printed Circuit Board of Analog Design proposed in Chapter - III.....	52
4.3. Laboratory Setup to Test Different Stages in Analog Circuit.....	53
4.4. Oscilloscope Screenshot for Amplifier Output Signal at 10Hz	54
4.5. Frequency Response of Implemented Low Pass Filter (fc = 100Hz)	55
4.6. Frequency Response of Implemented High Pass Filter (fc = 0.5Hz)	56
4.7. Frequency Response of Implemented 60Hz Notch Filter.....	57
4.8. Oscilloscope Output of DC Bias Filter indicating Mean Voltage of Signal	58
4.9. Frequency Response of Implemented DC Bias Filter.....	59

List of Figures—continued

4.10. Frequency Response of Implemented Analog Circuitry on PCB	60
4.11. Phase Difference (Time Delay) between the Input and Output Signals for Analog Circuit at 20Hz	61
4.12. Frequency Response Comparison to the Designed and Implemented Circuits	62
4.13. MSP-EXP430F5438 Experimenter Board.....	64
4.14. PAN1323 Evolution Module Kit for Bluetooth Operation.....	65
4.15. Hardware Interconnections between MSP-EXP430F5438 and PAN1323EMK.....	66
4.16. ADC Conversion Result Shown on LCD for 1.5 V DC Signal	68
4.17. ADC Conversion Result Shown on LCD for 2.5 V DC Signal	69
4.18. Configuration of Experimenter Board	71
4.19. LCD Indication of Bluetooth Menu on Board Startup.....	72
4.20. LCD Indication of Turning ON Bluetooth & Device Visibility	73
4.21. LCD Indication of Bluetooth Devices with SPP upon Discovery	73
4.22. LCD Indication of Successful Device Connection	74
4.23. LCD Indication of Data Transfer to Connected Device	74
4.24. Graphical User Interface of ‘EEGscope’ App on Android	76
4.25. Screenshot of ‘EEGscope’ Scan for Available Devices	76
4.26. Screenshot of ‘EEGscope’ Connection Status with ‘EEGBF58’	77
4.27. Real Time Plotting of Received Data per 1 Second Interval on ‘EEGscope’	78
4.28. Setup of Designed Prototype for EEG Acquisition System used on a Subject.....	79

List of Figures—continued

- 4.29. Display of Received EEG Signals on the ‘EEGscope’ Android App..... 80

CHAPTER – I

INTRODUCTION

An electro encephalogram [EEG] is a recording of the voltage potential developed across the human scalp due to iconic transfer between the neurons of brain cells during its activity. These potentials are recorded from different regions of the scalp for which each region has got its own importance as they depict the neuronal activity at different locations of the brain. [1-3]

These potentials would be in the range of $10\mu\text{V}$ to $100\mu\text{V}$ when collected using the external electrodes attached to the scalp [3]. Also noise from the surrounding tissues of the body and interference from the nearby electrical sources is added to the electrode voltages. Hence, preprocessing of collected signal is necessary.

Initially with the advent of the EEG recording systems, the signal collected from the electrodes was preprocessed for amplification and noise removal using the analog circuitry and then transferred to the computer using RS232 or Ethernet interfaces via wires [1] as shown in figure 1.1. Due to the latest technology advancements in the medical device field and advent of the wireless transmission protocols and the demand on home care of patients, the EEG acquisition systems [4-7] are considered for wireless transmission using technologies such as Bluetooth, Zigbee and RFID etc. onto a computer for data analysis and feature extraction.

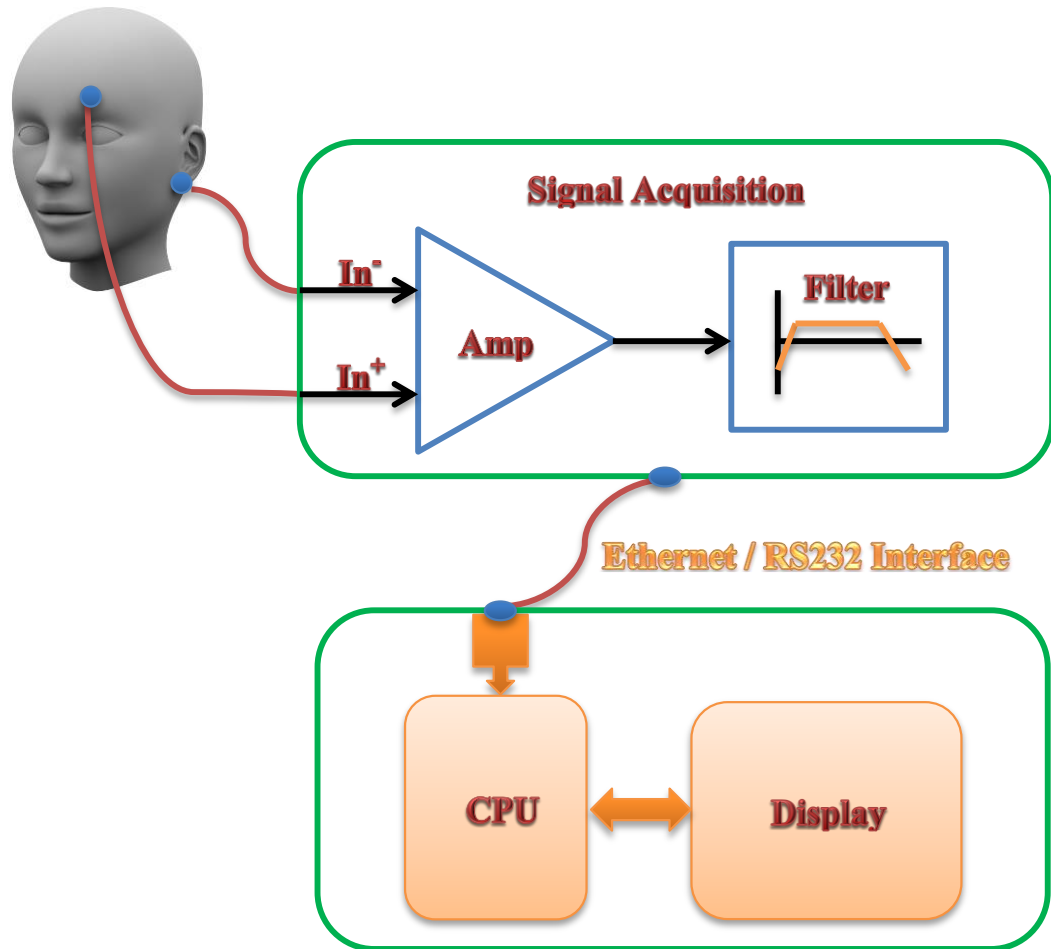


Figure 1.1. General EEG Acquisition System [1]

Due to the increased health care costs and aim to provide quality health care, there is extensive ongoing research to develop the portable instruments needed to acquire the signals and transmit them to the automated systems which constantly monitor patient. At times there is a need to provide urgent care for the patient under supervision exercising daily activities when suddenly affected from disorders such as seizures by alerting health care providers. There is no such system reported so far which is portable and creates alerts when needed. Hence an attempt has been made in this work to develop a prototype system that collects the EEG signal from the human subject and transmits onto a mobile

platform for analysis of required parameters, decision declaration and automated alerts to health care providers.

Ultimately we aim to have a system that is a patient monitor that has the ability to alert urgent care personnel of an abnormal neurological activity which vary based on the specific disorder. This project aimed for the development of a prototype system which includes analog circuitry for preprocessing and digital circuitry for transmission onto the android platform of a mobile. The preprocessing and preconditioning circuit is designed to perform the amplification of the raw EEG signal obtained using electrodes and noise removal, regardless of source being the bodily tissues and electrical interferences. The digital circuit is designed to carry on the analog to digital conversion and transmission of the sampled data into the Bluetooth module using a microcontroller. Finally, the Bluetooth module broadcasts the signal to the device which is connected to it via the Bluetooth radio. A specially designed software application that has the capability to communicate and control the Bluetooth hardware of the mobile phone is used to receive the signal from the prototype instrument.

The rest of this thesis is organized as follows: Chapter 2 provides the background theory related to the bio-potential signals and medical instrumentation development while chapter 3 describes the design procedure for the prototype system. In Chapter 4, we present a discussion of the implementation procedures and challenges and analysis of the acquired data. Chapter 5 provided conclusions and suggests the future work that can help to improve and extend the current design.

CHAPTER – II

PERTINENT LITERATURE AND BACKGROUND

2.1. Bioelectric Potentials

These are potentials developed due to the difference in electric fields on the inner and outer environments of cells that belong to the nervous and muscular systems. These cells are called excitable cells [1]. They exhibit a resting state potential when are at rest and action potentials when stimulated. The resting state potential of inner medium of these excitable cells is in the range of -50mV to -100mV with reference to external environment.

The reason for this potential difference is due to interchange of ions across the cell membrane. The cell membrane is made up of lipoprotein complex and looks very thin in size (7-15nm). The lipoprotein complex does not allow or impermeable to the intracellular compounds or the surrounding ions. But, the cell membrane in resting state is permeable to the Sodium (Na^+), Potassium (K^+) and Chlorine (Cl^-) ions which easily flow across the membrane (Movement Artifact) based on their individual electrochemical properties. Due to the difference in ion concentration between the inner and outer media of cell membrane, the above said ions travel across the membrane till an equilibrium state is obtained where the current is zero across membrane [2]. The high permeability of the Potassium ions makes them to travel in high quantities creating a negative potential on the inner side of membrane. The expression for the equilibrium resting potential is given by equation 2.1.

$$E = \frac{RT}{F} \ln \left\{ \frac{P_k[K]_o + P_{Na}[Na]_o + P_{Cl}[Cl]_i}{P_k[K]_i + P_{Na}[Na]_i + P_{Cl}[Cl]_o} \right\} \quad (2.1)$$

Where E is the equilibrium trans membrane potential, R is the universal gas constant, T is the absolute temperature, F is the Faraday constant, P_M is the permeability constant of ion 'M' in moles per liter and $[M]_o$ and $[M]_i$ are the extracellular and intracellular concentrations of the ion 'M'.

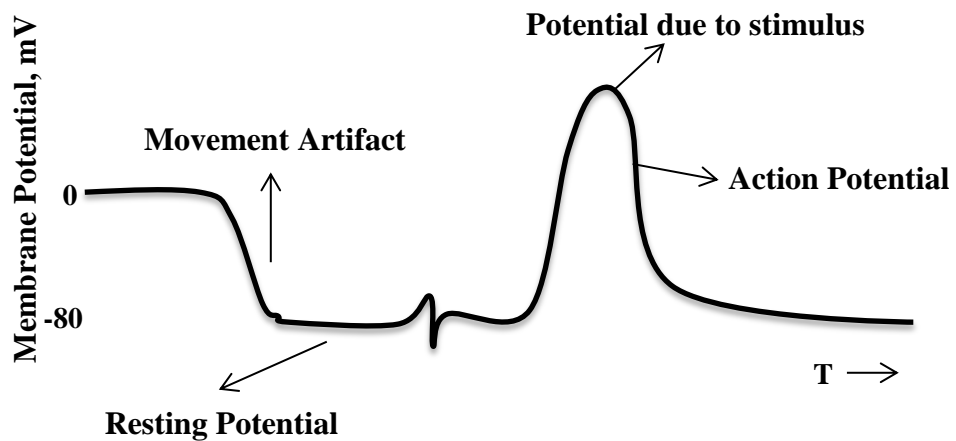
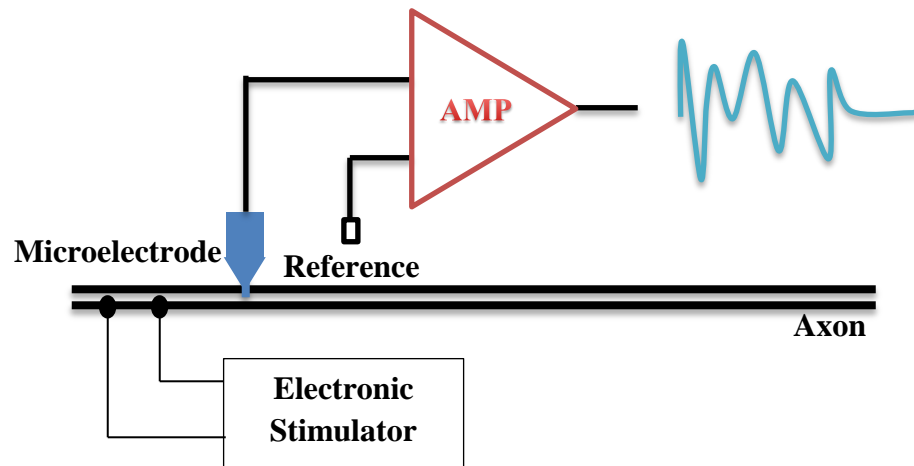


Figure 2.1. Recording and Interpretation of Action Potential of Cell Membrane [1]

During the active state, the cell membrane conducts the active potential due to the adequate stimulus. The magnitude and time of the active potential changes the permeability properties of the cell membrane and thereby the ion transfers takes place

[2]. A difference in the cell membrane potential is observed as a result of this stimulus and the cell membrane returns to its equilibrium potential when there is no stimulus.

As shown in figure 2.1, the cell membrane potential can be recorded by using the micro electrodes penetrating into the tissue and touching the cell membrane [2]. These recordings can be correlated to many known and unknown specifications of the tissues from which they are collected and use them appropriately either for the clinical diagnosis applications or the intelligent controls system design.

2.2. Electroencephalography

Due to ionic transfers during the neuronal activity in brain cells, an electric potential is developed in the neurons. This combined voltage potential from multiple neurons can be measured from different locations of the scalp. This recording of the neuron potential is referred to as Electroencephalogram [1-3]. These potentials depend on the physiological and functional state of the brain. The anatomy of the brain is shown in figure 2.2.

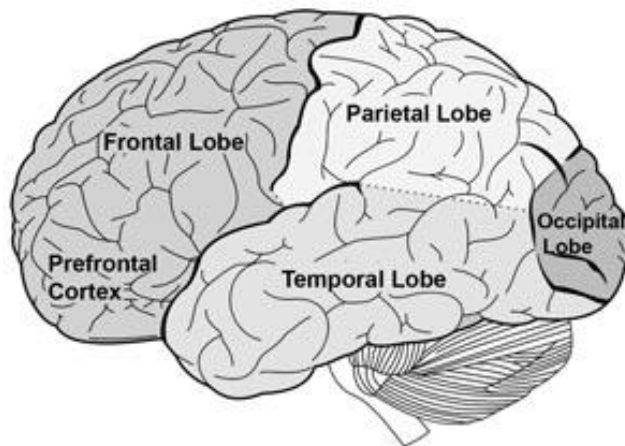


Figure 2.2. Anatomical Structure of Brain [3]

Brain is the main functional organ in human body which controls every action of the body. The brain is basically divided into left hemisphere and right hemisphere. The right hemisphere controls the left side of the body and performs the activities related to artistic and creative ability whereas the left hemisphere controls the right side of the body and performs the activities related to speech, reading, writing and logical thinking. Based on these functionalities, brain is divided into different regions as listed in table 2.1.

Table 2.1. Significance of Anatomical Regions of Brain as Shown in Figure 2.2. [3]

Region	Activity
Frontal	Speech, Thought, Emotion, Problem Solving and Skilled Movements.
Parietal	Identifies and interprets sensations such as touch, pain etc.
Occipital	Collects and interprets visual images i.e. sight.
Temporal	Hearing and Storing Memory.
Cerebellum	Controls and Coordinates familiar movements.

The voltage waveforms recorded from the normal activity of the brain are classified into different frequency bands and their generalized location of origin is summarized in table 2.2.

Delta waves occur when the subject is in deep sleep, in infancy and suffering with serious organic brain disease. Theta waves mostly occur in infants and sleeping adults. Alpha waves are the most general type of brainwaves found in adults in the normal state of rest and relaxation. Beta and Gamma waves are observed when the subject is undergoing the state of intense mental activity in brain. The waves with higher

frequencies are observed when there is any disorder in physiological state of brain or when the subject is suffering from disease related to brain.

Table 2.2. Types of Brainwaves [1-7]

Type	Frequency Range	Origin
Delta	0Hz – 4Hz	Cortex
Theta	4Hz – 8Hz	Parietal and Temporal
Alpha	8Hz – 13Hz	Occipital
Beta	13Hz – 20Hz	Parietal and Frontal
Gamma	20Hz – 40Hz	Parietal and Frontal

2.3. Medical Instrumentation System

This section describes the knowledge that an engineer should have before developing a medical instrumentation system which can be represented by the following block diagram [1, 2, 9] shown in figure 2.3.

In the figure 2.3 the steps shown with the solid arrows are compulsory and rest of them are needed based on the necessity and requirement. The measurand which is a physical quantity that can be collected either from inside the body or from surface of the body, stimulated internally or by an external media and collected by the sensor is analyzed by the appropriate signal processing algorithms either in analog or the digital domain and displayed in the permeable output unit. The data after collection is passed through the signal conditioning phase either to amplify or to filter by applying various signal processing algorithms and can be stored in the digital medium to transmit onto a platform where a microcomputer is utilized for advanced signal processing and

interpretation algorithms. The processed signal can also be given as a combinational feedback to the sensing element.

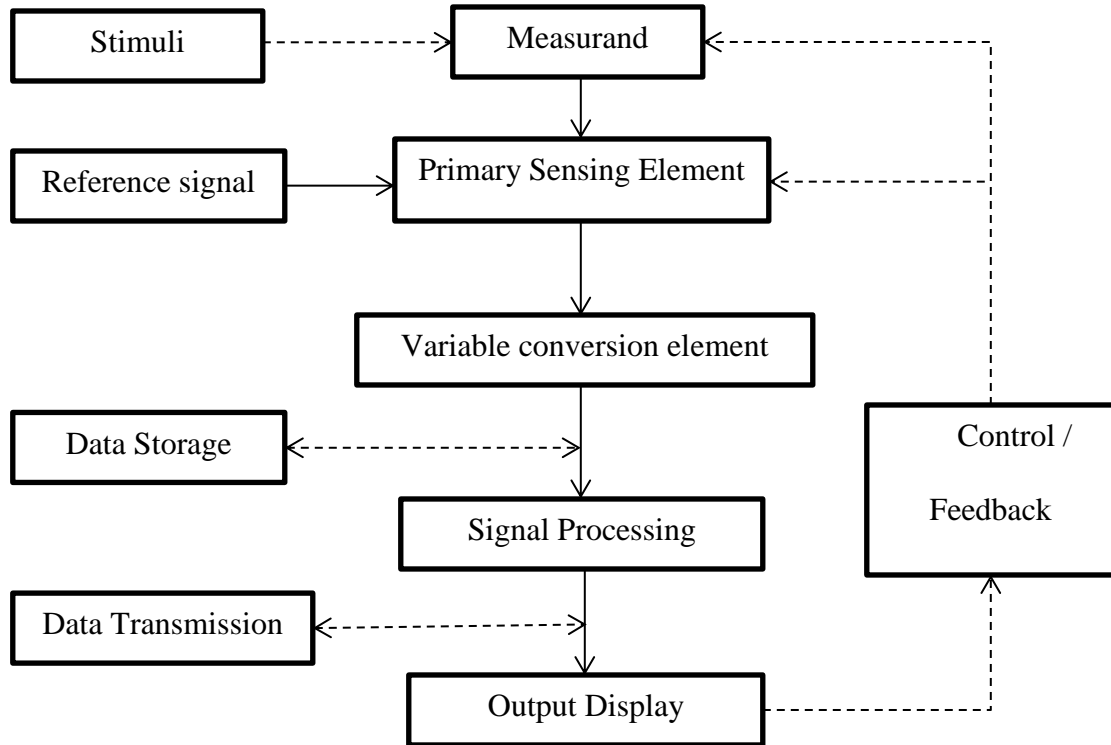


Figure 2.3. Generalized Medical Instrumentation System [1]

2.4. Bio-Potential Electrodes

These are the electrodes which provide an interface between the body and electronic instrumentation to measure and record the potentials by conducting the current across the interface. The current in the body is carried by the ions whereas the current in the electrode is carried by the electrons and hence there is a charge transfer at the interface as per the below expressions [2] and the charge transfer between the electrode – electrolyte interface is shown in figure 2.4.

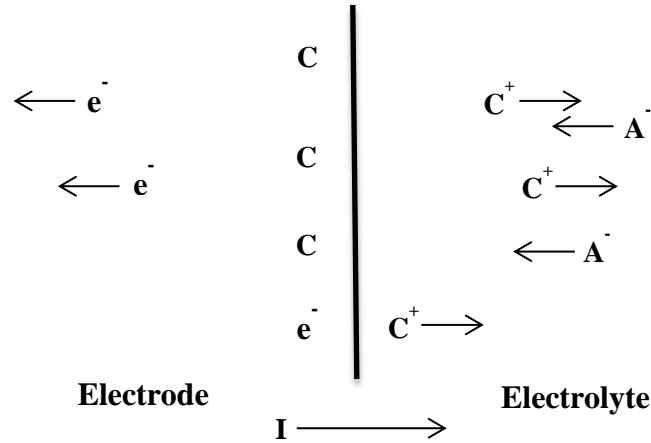


Figure 2.4. Ion Exchange at Electrode Electrolyte Interface [2]

The electrode contains the metal atoms ‘C’ whereas the electrolyte contains the cations of metal ‘C⁺’ and anions ‘A⁻’. For the current flow from electrode to electrolyte, the metal atoms oxidize to split into cations which diffuse into the electrolyte and anions reduce by combining with electrons after diffusing into the electrode. This is how the charge is transferred across the interface and results in flow of current in the direction of higher rate of diffusion. The net current would be zero if the rate of oxidation and reduction are equal. The different types of body surface recording electrodes that can be used for patient monitoring application and their significant uses are furnished in the table 2.3.

Most of the surface electrodes are manufactured using the silver/silver chloride metals due to its non-polarizable characteristics and ease of fabrication. These are

manufactured by inserting a silver metal base connected to an insulated lead wire into an electrolyte solution with large concentration of anions (Cl^-) and thereby allowing a chemical reaction (Electrolysis) to precipitate silver chloride (AgCl) on the silver base. The AgCl is very little soluble in water and hence it is very stable in the electrolyte medium. Apart from the above characteristics, the Ag/AgCl electrodes will have low electric noise and high impedance at the low frequencies due to capacitive behavior at the electrode-electrolyte interface.

Table 2.3. Types of Surface Recording Electrodes [3]

Electrodes	Contact Type	Significant Usage
Metal Plate Electrodes	A metallic conductor in contact with skin with the help of an adhesive electrolyte gel	limb electrodes for ECG
Metal Disk Electrodes	A metallic disk applied to skin with a surgical tape.	Chest electrode for ECG, surface recordings of EMG, EEG etc.
Suction Electrodes	A metalling electrode placed on the skin with the help of rubber suction bulb.	Precordial electrodes for clinical ECG
Floating Electrodes	A cavity filled with the electrolyte gel is placed on the skin in which the electrode is at the bottom of cavity.	Reduces the motion artifact between the skin and the electrolyte gel.
Flexible Electrodes	Flexible electrode which can easily fix to any topography.	Mostly used in the premature infants

2.5. Bio-Potential Amplifiers

An amplifier is an important and most commonly used part of the medical instrumentation system. The bio-potential signals that are collected from the human body possess very low amplitudes and hence are needed to amplify in order to process, analyze and display them. The amplifiers used for this purpose are often called bio-potential amplifiers. These amplifiers had to meet certain specifications [2] to record the bio potential signals without any distortion. They are:

1. High Input Impedance.
2. Reverse current protection.
3. High Gain.
4. Low Frequency operation.
5. High Common mode rejection ratio (CMRR).

These amplifiers need to have high input impedance so as to reduce the loading effects of electrodes which reduce the amplitude of signal being collected. Hence to reduce the loading effects, the bio potential amplifiers need to have input impedance as large as possible. The latest bio potential instrumentation amplifiers have an input impedance of around $10M\Omega$ [1]. These amplifiers should also have an ability of providing protection to the subject under study from reverse current. The currents from the input terminal of the amplifiers can cause micro shocks to the patient in clinical studies. Hence the bio-potential amplifiers needed to have a protection circuitry at the input so as to maintain safe current levels through the electrodes.

Apart from above parameters, the bio-potential amplifiers should have high gain in the order of 1000 as they deal with signals of ultra-low amplitude range i.e. micro volts

range which are to be amplified to facilitate the application of signal processing algorithms for its analysis. Also these amplifiers should operate in the frequency range of the bio-potential signals which are at low frequency range close to DC signals. During the bipolar acquisition of bio potential signals with common reference, there is a possibility of common mode voltage greater than the amplitude of the signal would show up which distorts the actual bio-potential signal. Hence the amplifier should have high CMRR ratio (typically $> 80\text{dB}$) to reject the common mode signal [1, 2]. These properties are necessary to analyze the signal strength and its integrity.

2.6. Analog Bio-Potential Signal Processing

Operational amplifiers play a major role for applying analog signal processing algorithms on the amplified signal. Apart from signal amplification, different combinations and topologies of these operational amplifiers are used for noise frequency removal and non-linear modification of signals. The operational amplifier is basically a differential amplifier which multiplies the difference signal between the two input terminals with a high gain [10] as shown in figure 2.5.

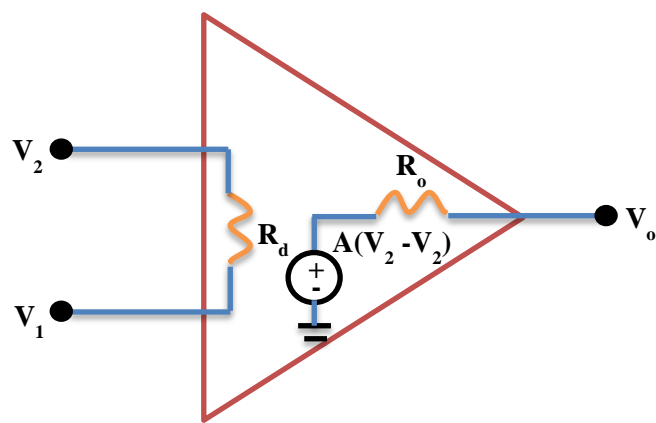


Figure 2.5. Op-Amp Equivalent Circuit [10]

The inverting and non-inverting amplifiers are basic building blocks for various kinds of amplifier configurations to modify or filter the signal as required. The figure 2.6 depicts these amplifier configurations with respective gains.

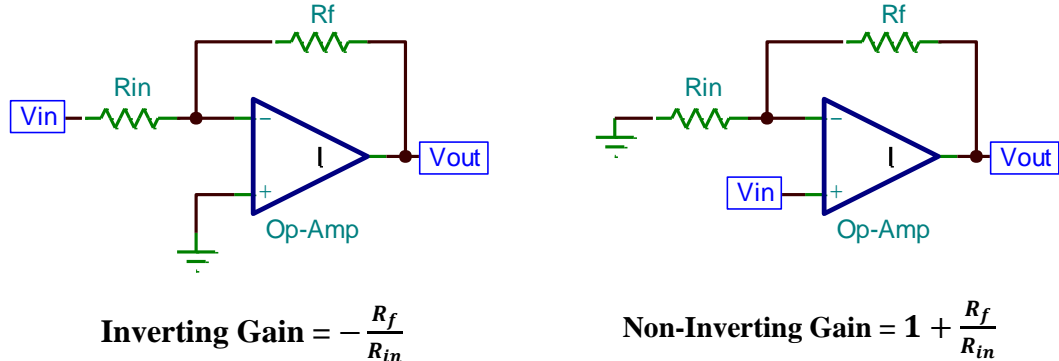


Figure 2.6. Inverting and Non-Inverting Amplifiers [10]

After acquiring the bio-potential signals via the electrodes, the bio potential amplifiers are used to amplify these signals and then filters are used to reduce the noise frequencies and obtain clear signals. The active filters i.e. the passive filters with an active feedback through the operational amplifier are designed to filter the known noise frequencies [2, 10].

The gain of the frequency filters varies with frequency. This is obtained by using the components of the amplifier circuit that vary their impedance values based on the frequency of signal. This is achieved by using capacitors along with resistors in the circuit. These filters are classified as Low pass, High pass, Band pass and Band reject filters. There would be a threshold frequency for each filter at which the gain of the filter is -3dB. This is also called the cutoff or corner frequency between the pass band and the stop band. So when a filter is designed one has to take care of the cutoff frequency so as to obtain the filter with accurate frequency response. Since it is known that the gain of the

filter depends on the ratio of the feedback impedance to the input impedance and impedance of capacitor is inversely proportional to the frequency, the capacitor is placed at input to obtain high gain at low frequencies and in feedback loop to obtain gain at high frequencies. The combination of low and high pass filters according to the requirements of cutoff frequencies would result in the band pass and band stop design of filters. The model and frequency response of these high pass and low pass filters are given in figures 2.7 and 2.8.

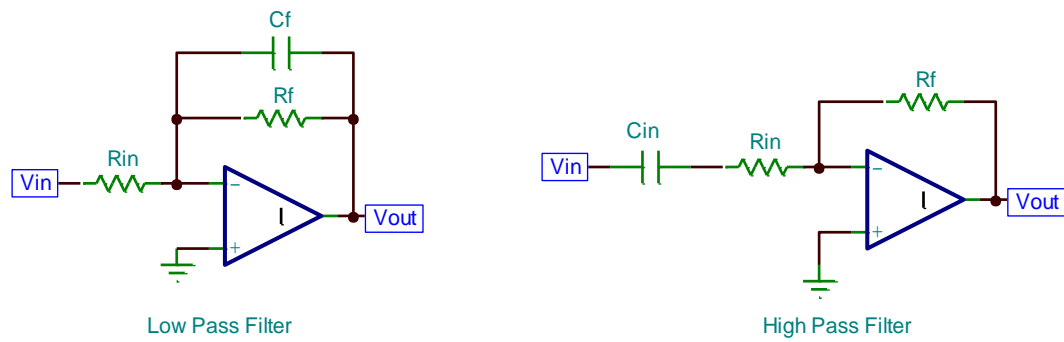


Figure 2.7. Active Frequency Filter Models [10]

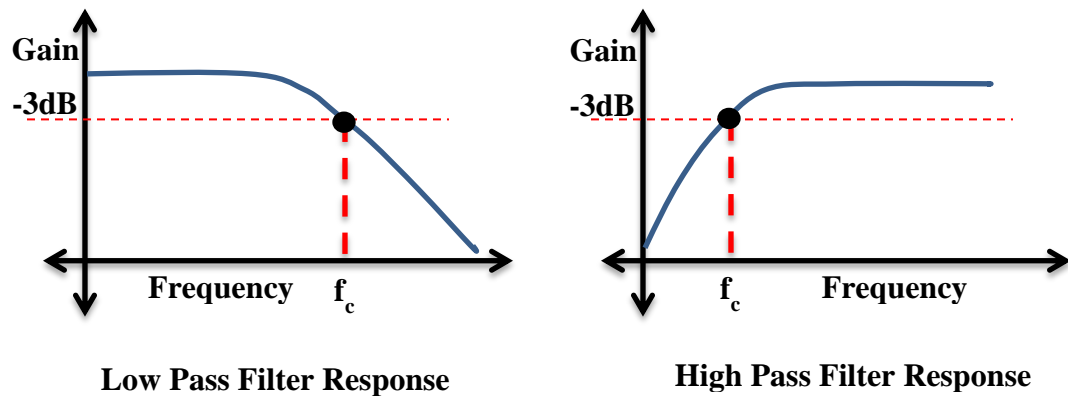


Figure 2.8. Frequency Response of Low Pass and High Pass Filters [10]

2.7. Digital Bio-Potential Signal Processing

The analog signal processing methods that we discussed so far can be implemented with large components and manual supervision. With the advent of digital electronics and microcomputers such as microcontrollers and microprocessors, most of these analog signal processing methods can be implemented by a single computer reducing the complexity of design. This facilitates the storage of data and feedback controls back to the system [1-3].

The analog signal has to be converted into digital signal before applying digital signal processing algorithms. This digital processing not only reduced the complexity of design but inherited decision property based on the analysis without a need for constant supervision. Hence usage of the microcomputers for signal processing in the medical instrumentation area increased the reliability of the instruments acquiring bio-potential signal either clinically or for in-laboratory experiments [1, 9].

By transmitting the digitally converted data onto a system which could be able to perform complex analysis algorithms, a lot of features in the digital signal are identified and extracted from these bio-potential signals which can be correlated with different parameters of the tissues from where they are acquired [3]. This analysis is performed in the specially designed software (Graphical User Interface) that can be interfaced with the acquisition hardware when connected to the computer [2].

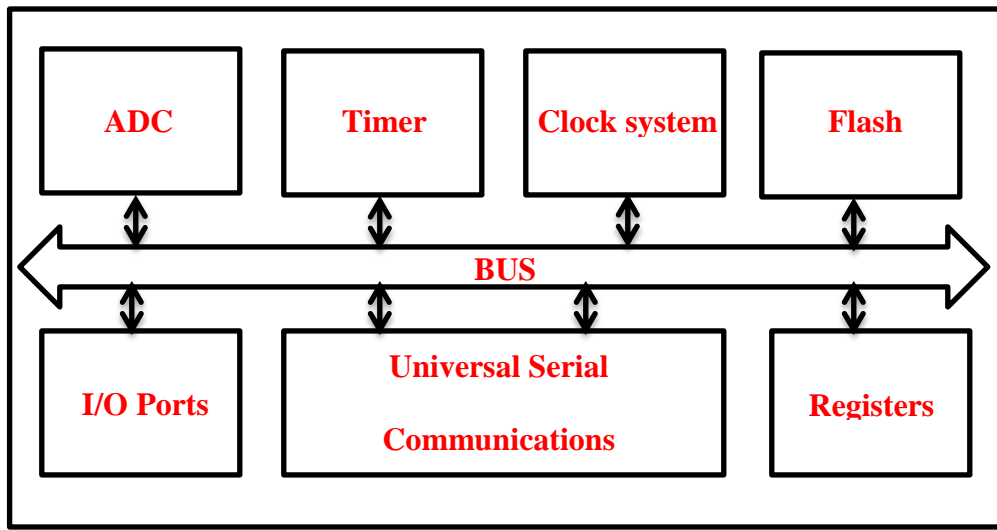


Figure 2.9. Microcomputers in Signal Processing [1, 9]

There are many microcontroller modules that are available in the market which can be used for the digital signal processing techniques and a general architecture of the microcontroller with some of those modules is shown in figure 2.9. A general microcontroller consists of many modules like timers, analog to digital converters, universal serial communication interfaces along with some special modules which vary with different kinds. These modules are collectively programmed by the computer to perform the anticipated analysis on the analog signals and provide automated controls based on the results. These results along with the data at different stages of processing can be displayed in the monitor connected to the controller.

2.8. EEG Acquisition Practices

There are many commercial devices that have been developed so far for the purpose of electroencephalogram recordings which are being used in various clinical applications [4-8]. Most of these applications use wired components that are attached to

the end devices where EEG or any other bio-potential signal analysis is done either to diagnose the patient or to convert the signal into control for Brain Machine Interfaces.

Figure 2.10 furnish the evolution trend of EEG acquisition systems starting from 1920's to late 2010's [1, 2]. It started with recording of EEG signals using galvanometers and micro electrodes in late 1940's. In course of time signals are analyzed with advanced digital signal processing algorithms for EEG pattern recognition and detection along with the development of Portable Instrumentation mechanisms.

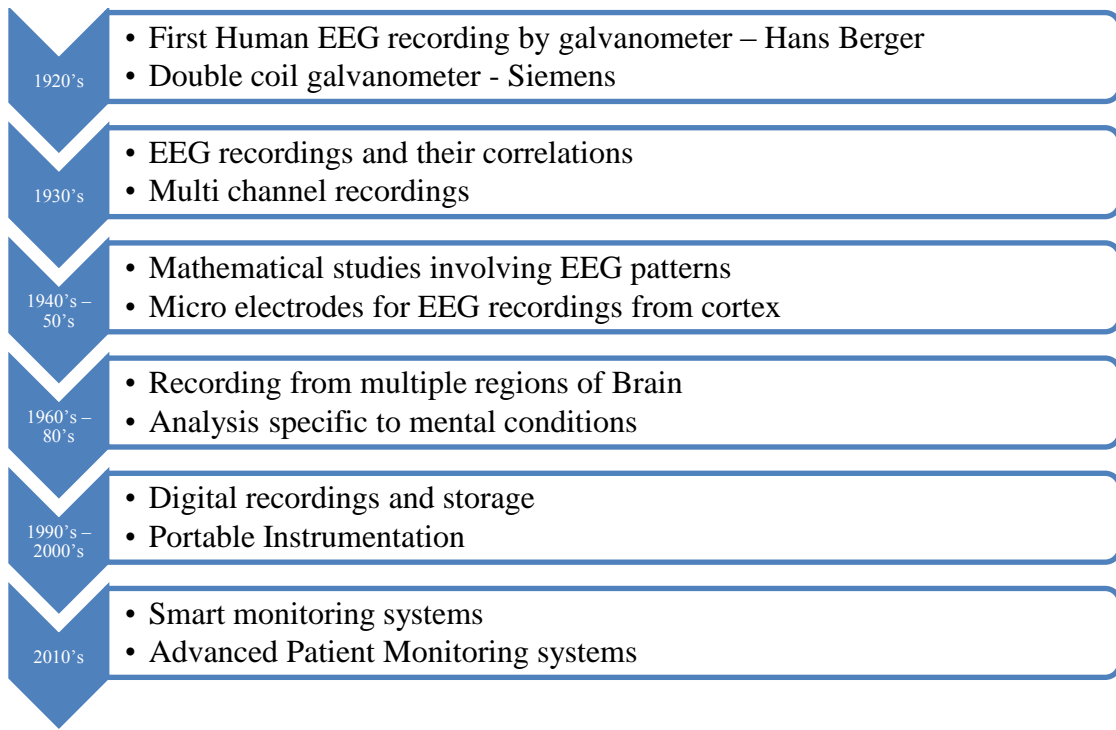


Figure 2.10. Evolution of EEG Recording Systems [1, 2]

Long-term research resulted in development of the portable devices [5] that can perform pre analysis of raw EEG signals collected from one of the locations specified in the International 10-20 placement system of electrodes around the scalp and store them electronically [2]. These electronic signals stored in the electronic drives were transferred into the system for analysis. With the advent of the wireless technologies [4-8] like Radio

Frequency Identification (RFID) and Bluetooth Connectivity, a real time analysis is performed on the acquired signals by wireless transmission into the system using the specially designed graphical user interface software developed for the analysis based on the application intended to use with.

One of the applications of these real time EEG acquisition systems is to monitor the patient suffering from clinical disorder related to the brain [4-7]. This requires the patient to be in the health care center under the constant supervision for diagnosis which results in the high costs. Hence these systems have to be optimized to use at any location and connected to an automation system which monitors the patient [12, 26]. One of the best known solutions is to develop a device that is capable of transmitting the signal to a mobile platform with data connectivity so as to establish the connection with automation system which constantly monitors the patient.

2.9. Smart Acquisition Systems

Today there is a large advancement in the technology that the smart operating systems are being utilized in many of the consumer electronics systems. These smart systems are also being developed in the medical instrumentation field so as to increase the effectiveness of the medical care and patient monitoring systems [9, 11, 12]. These smart acquisition systems facilitate the health care provider to constantly monitor the patients with ease and interactive graphical user interface which can perform the desired analysis without the use of PC.

The most successful operating system is the Android operating system [11] due to its feasibility to develop applications with user friendly graphical interface that can work with wide varieties of hardware connected to it. This android software is developed using

Java language and many examples are provided by the android developers for the beginners to develop the software applications.

This design aims to develop an application connected to the Bluetooth hardware of the Android operated mobile (Android 2.0 or high) that is capable of receiving signals from the nearby Bluetooth devices. The Sample projects [24] that are provided as part of the Android software development kit and the Bluetooth applications [25] that are available in the Android market store are carefully studied to understand the creation of the applications on android.

2.10. Summary

This chapter explains the significance of electroencephalograms and their classification based on the frequency and origin, the development of medical instrumentation systems and the role of operational amplifiers in the preprocessing of analog signals before analyzing them in digital domain for advanced analysis and the evolution of smart systems in the medical instrumentation arena.

CHAPTER – III

SYSTEM DESIGN - HARDWARE AND SOFTWARE

3.1. Introduction

This section describes the design of pre-conditioning circuit, digital circuit for transmission and android graphical user interface design which are interfaced to develop the prototype system as shown in figure 3.1.

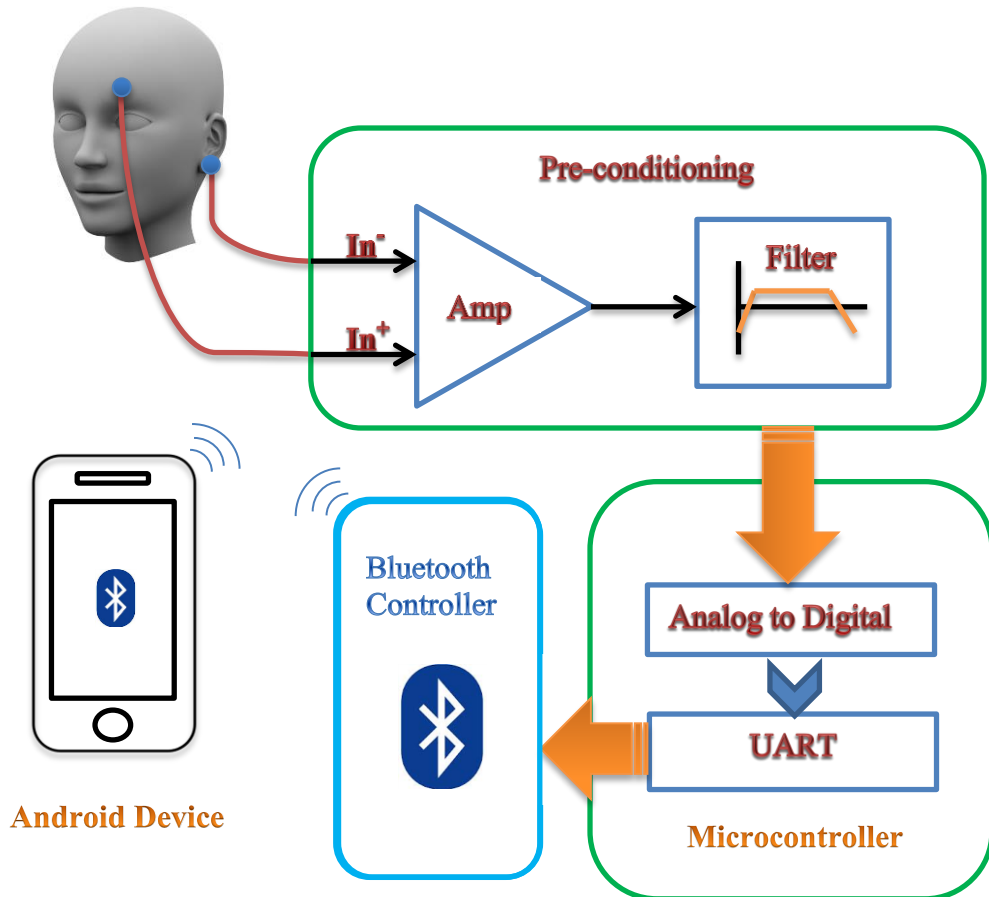


Figure 3.1. Block Diagram of EEG Acquisition System

From figure 3.1, the pre conditioning circuit consists of an amplifier and the filter to remove noise and amplify the signal before feeding into the micro controller for A/D

conversion. The digital circuit consists of the micro controller for analog to digital conversion and transmits the digital data to Bluetooth module coupled to it via Universal Asynchronous Receiver/Transmitter (UART) interface. An android application is developed to receive the signal on the mobile.

3.2. EEG Signal Acquisition

In order to measure and record the potentials from the body, it is necessary to provide interface between body and potential measuring electronics apparatus. The EEG signal form the brain is acquired using electrodes placed on the scalp region of head.

The typical electrodes used for this acquisition are made up of Silver-Silver Chloride [1, 2] and are manufactured by many companies in different kinds as shown in figure 3.2. The Ag-AgCl electrodes are used in the EEG signal acquisition since they have low impedance, low offset voltage and low noise with high stability. The application or preparation gel is needed for preparing the skin before attaching electrodes to the skin which reduces input impedance and helps for smooth conduction of the current through electrode – electrolyte interface.



Figure 3.2. Ag-AgCl Electrodes (Flat and Ear clip) used for EEG Acquisition

When these conductive gels lose its adhesion then the problem arises with increased input impedance which decreases the signal to noise ratio of electrode - electrolyte interface. In this design the EEG signals are collected at the forehead region with earlobes as the reference.

3.3. Amplifier Design

The signals obtained from the electrode leads are about $1\mu\text{V}$ to $100\mu\text{V}$ range which are of very low amplitude range and hence are very difficult to analyze these signals. They have to be appropriately amplified so as to perform analysis which in turn depends on the hardware utilized for this purpose. So the amplifier gain should be around 5000 to 10,000 based on the signal amplitude range.

The instrumentation amplifier is employed because it has high input impedance and high CMRR ratio. Common mode rejection ratio (CMRR) is the ability or tendency of the amplifier to reject the similar voltages common to both inputs. The high CMRR ratio is very necessary because the input voltage swing from the electrodes is very less in the range of few micro volts [1, 2]. CMRR ratio is given by the ratio of differential gain to the common mode gain.

For this amplification stage the instrumentation amplifier INA128 [13] is selected from Texas Instruments. It is specially designed for the medical instrumentation applications where it has high input impedance that is required for transferring of voltages from electrode terminals with the internal over voltage protection circuit. It had a high common mode rejection ratio of 120dB [13]. The schematic of the selected amplifier to which the electrodes are connected is shown in figure 3.3.

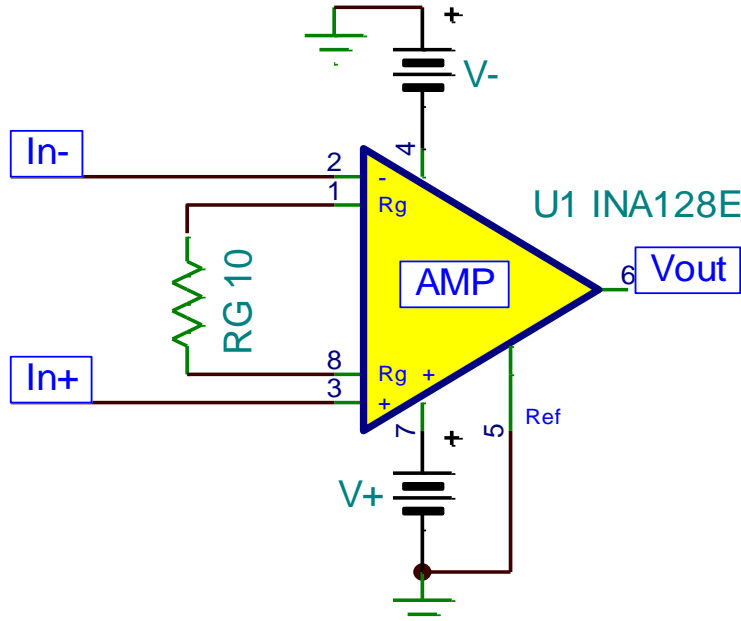


Figure 3.3. Schematic of the INA128 Instrumentation Amplifier Circuit [13]

The expected gain from the amplifier is up to the range of 10,000 which is based on the value of the Gain Resistor (R_G) commonly connected to the inverting terminals of the first two operational amplifiers inside the instrumentation amplifier INA128. Its feasibility to the high temperature and its low input power supply of 2.4V makes it suitable for the portable instrumentation with the effective power management using low power supplies. The gain equation for the INA128 instrumentation amplifier is given by equation 3.1. [13]

$$G = 1 + \frac{50k}{R_G} \quad (3.1)$$

Since the desired signal should be in the range of $\pm 1V$ and maximum voltage that can be obtained from the electroencephalogram is about $200\mu V$, the gain resistor used in this design is 10Ω for which the amplifier yields the gain around 5000 V/V or 74dB .

3.4. Active Filter Design

The frequency range of the EEG signals for the normal human adult subject will be of 1Hz to 40Hz and it may extend up to 100 Hz based on the abnormal functionality of the brain [1-3]. In the acquisition of the EEG signals there will be interferences from sources of different origins which can be from surroundings or within the body. The noise from the internal tissues is contributed by the potentials developed across them interfering with recordings at the surface. These signals will generally be of high frequency more than 100Hz. Also the environmental artifacts due to the surroundings including DC offsets from electrical instruments will be observed in the low frequency range with the mean frequency of 0.5 Hz. The interference due to the AC electrical lines is at 60Hz which is also a source of noise.

Hence it is necessary to preprocess using a filter which is capable of eliminating all interference signals. The required filter is obtained by cascading the sub-filters each designed to meet desired specifications. The filter needed to have a flat frequency response with sharp transition in the cut-off region. This can be achieved by designing a filter of Butterworth type which will have a flat frequency response in the pass band region and sharp transition at the cut-off region which increases with order of filter. The filter is designed by cascading the Low Pass filter ($f_c = 100\text{Hz}$), High Pass filter ($f_c = 0.5\text{Hz}$), Notch filter ($f_c = 60\text{Hz}$) and DC Bias filter. The block diagram of the filtering stage designed with sub filters is shown in figure 3.4.

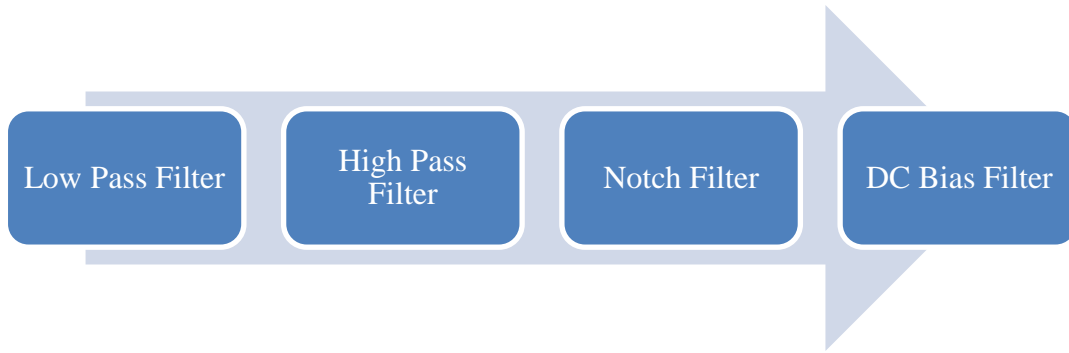


Figure 3.4. Block Diagram of Active Filter in the Analog Front End Design

The amplitude gain needed for the analysis of the EEG waves is obtained in the pre amplification stage since only the positive voltage can be given to the input terminals of the micro controller with a maximum value of 2.5V. And hence the active filter is to be designed for the gain of unity (0 dB) to allow the amplitude to be in the maximum allowable range. These filters are designed using the operational amplifiers that are available in the market. The operational amplifiers TLV2264 [14] from Texas Instruments Inc. and LM258 [15] from STMicroelectronics are chosen for implementation of sub filters in this project.

The basic design of the sub-filters follow the guidelines specified in the Active Filter Design [16] by the Texas Instruments Inc. using the Sallen-Key Topology shown in figure 3.5. The Impedances for the unity gain Sallen-Key topology are selected accordingly based on the frequency and the type of filters to be implemented i.e. Z_1 and Z_2 are resistors, and Z_3 and Z_4 are capacitors for Low Pass Filter and resistors and capacitors are interchanged for the High Pass Filter for the impedances shown in figure 3.5.

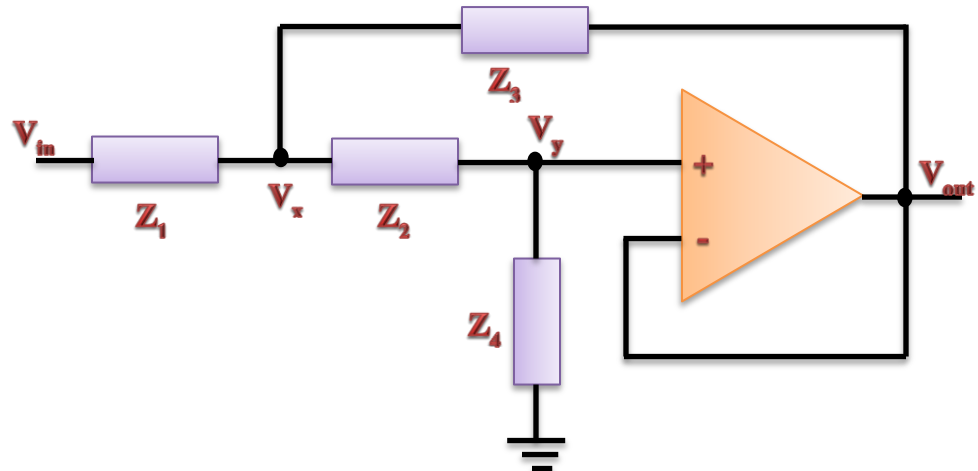


Figure 3.5. Second Order Unity Gain Sallen-Key Topology [16]

From figure 3.5, by Kirchhoff's current law, the currents at the nodes V_x and non-inverting terminal V_y are obtained as

$$\frac{v_{in} - v_x}{Z_1} = \frac{v_x - v_{out}}{Z_3} + \frac{v_x - v_y}{Z_2} \quad (3.2)$$

$$\frac{v_x - v_{out}}{Z_2} = \frac{v_y}{Z_4} \quad (3.3)$$

Also by assuming the ideal behavior of operational amplifier, the terminal voltages are equal and hence

$$v_y = v_{out} \quad (3.4)$$

From the above three equations the transfer function can be obtained as

$$\frac{v_{out}}{v_{in}} = \frac{Z_3 Z_4}{Z_1 Z_2 + Z_3 (Z_1 + Z_2) + Z_3 Z_4} \quad (3.5)$$

3.4.1. Low Pass Butterworth Filter

A general Low Pass Filter will have a transfer function [10, 16] of

$$A(s) = \frac{A_o}{\prod(1 + a_i s + b_i s^2)} \quad (3.6)$$

The ‘ a_i ’ and ‘ b_i ’ are the ‘ i^{th} ’ stage first and second order filter coefficients which depend on the type of filter to be implemented. The second order Sallen-Key topology for the unity gain low pass filter is shown in figure 3.6. The generic expression for the Quality Factor of a filter with known filter coefficients is $Q = \frac{\sqrt{b_i}}{a_i}$ which specifies the damping nature of the filter.

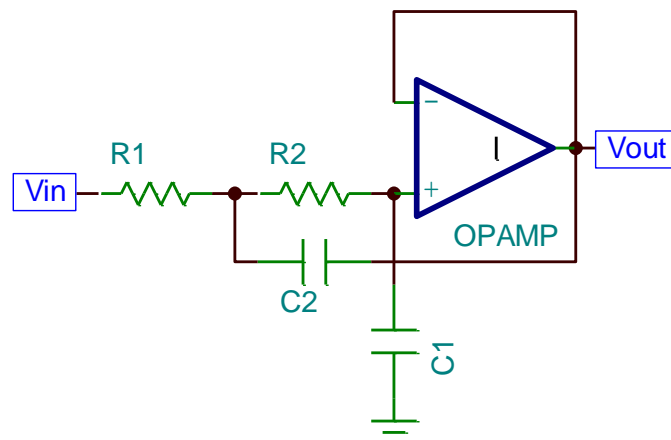


Figure 3.6. Sallen-Key Topology of Unity Gain Low Pass Filter [16]

The transfer function of the Low Pass filter is obtained by replacing the impedance values with the corresponding Laplace transforms i.e. R for the resistor and $1/sC$ for Capacitor in the equation 3.5.

$$A(s) = \frac{1}{1 + \omega_c C_1 (R_1 + R_2)s + \omega_c^2 R_1 R_2 C_1 C_2 s^2} \quad (3.7)$$

And the cut-off frequency, ω_c of the low pass filter is given by $\frac{1}{\sqrt{R_1 R_2 C_1 C_2}}$

By comparing the equation 3.7 with the generalized transfer function of the low pass filter, the filter coefficients and the gain are given by

$$A_o = 1 \quad (3.8)$$

$$a_i = \omega_c C_1 (R_1 + R_2) \quad (3.9)$$

$$b_i = \omega_c^2 R_1 R_2 C_1 C_2 \quad (3.10)$$

For the known filter type and desired cut-off frequency, the component values can be found from the above equations by knowing either the capacitor values or the resistor values. Hence in this design the standard capacitor values are assumed and the corresponding resistors are found out by solving known filter coefficients for the Butterworth filter. Hence the resistor values are given by

$$R_{1,2} = \frac{a_i C_2 \mp \sqrt{a_i^2 C_2^2 - 4b_i C_1 C_2}}{4\pi f_c C_1 C_2} \quad (3.11)$$

To obtain a filter with a flat frequency response and sharp transition region at 100Hz cut-off frequency, a multiple order filter is needed. After multiple implementations of the filter in the Pspice circuit simulation software using the above assumptions and equations, a 6th order Butterworth filter is identified with required performance in the pass band region with unity gain and -3dB gain at the cut-off frequency of 100Hz. Though we could obtain steeper transition in the cut-off region, to minimize the number of components (which is required for Portable Instrumentation) the order of filter is confined to 6. The filter coefficients are inherited from the standard filter design practices specified in the literature from Texas Instruments Inc. [16]. The schematic of the designed low pass filter is shown in figure 3.7.

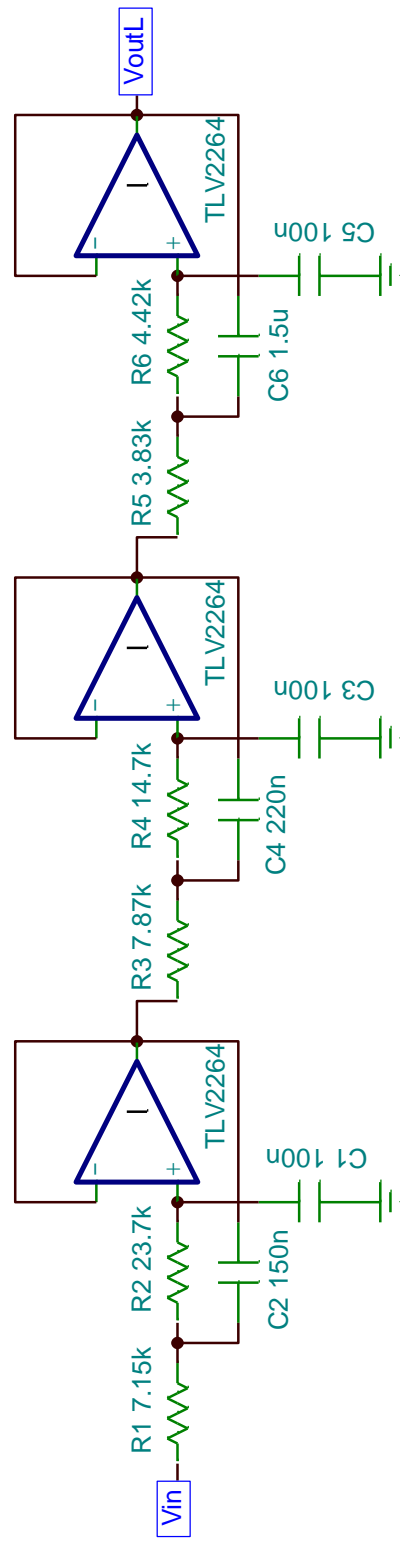


Figure 3.7. Designed 6th Order Low Pass Butterworth Filter

As shown in figure 3.7, the 6th order low pass Butterworth filter is designed by cascading the three 2nd order filters with known filter coefficients and standard capacitor values by calculating the resistor values. The table 3.1 shows the various component values assumed and calculated using equations 3.7 to 3.11

Table 3.1. Low Pass Butterworth Filter Specifications

Spec.	Stage-1	Stage-2	Stage-3
1st Order filter coefficient, a_i	1.9319	1.4142	0.5176
2nd Order Filter Coefficient, b_i	1	1	1
Capacitor, C_1	0.1μF	0.1μF	0.1μF
Capacitor, C_2	0.15μF	0.22μF	1.5μF
Resistor, R_1	7162.699Ω (7.15KΩ)	7864.996Ω (7.87KΩ)	3840.366Ω (3.83KΩ)
Resistor, R_2	23600.039Ω (23.7KΩ)	14654.111Ω (14.7KΩ)	4401.731Ω (4.42KΩ)
Quality Factor, Q_i	0.52	0.71	1.93
Frequency Ratio, K_i	0.676	1	1.479

For implementation, the standard resistor values of 1% tolerance, standard capacitor values of 20% tolerance and TLV2264 [14] operational amplifier are considered based on feasibility. The simulated frequency response of the designed low pass filter from the Pspice circuit simulation software is given in figure 3.8 which indicates the -3dB gain at 100Hz.

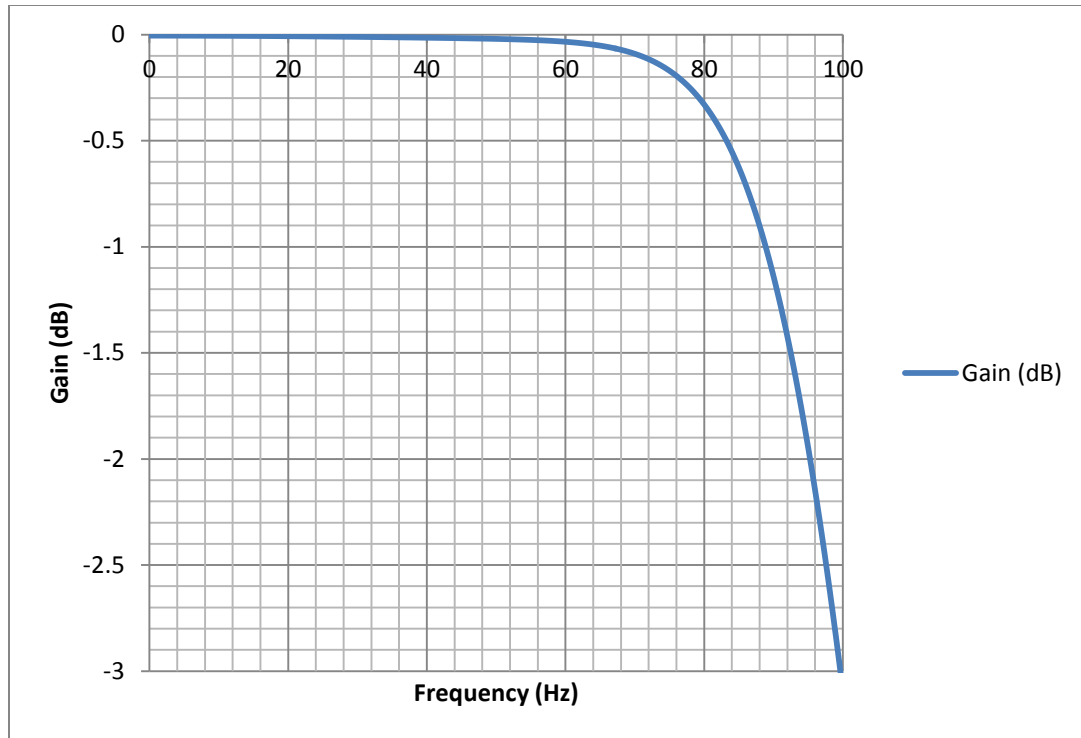


Figure 3.8. Simulated Frequency Response of Designed Low Pass Filter on Pspice

3.4.2. High Pass Butterworth Filter

A general High Pass Filter will have a transfer function [10, 16] of

$$A(s) = \frac{A_{\infty}}{\prod \left(1 + \frac{a_i}{s} + \frac{b_i}{s^2} \right)} \quad (3.12)$$

The ' a_i ' and ' b_i ' are the ' i^{th} ' stage first and second order filter coefficients which depend on the type of filter to be implemented. The second order Sallen-Key topology for the unity gain high pass filter is shown in figure 3.9.

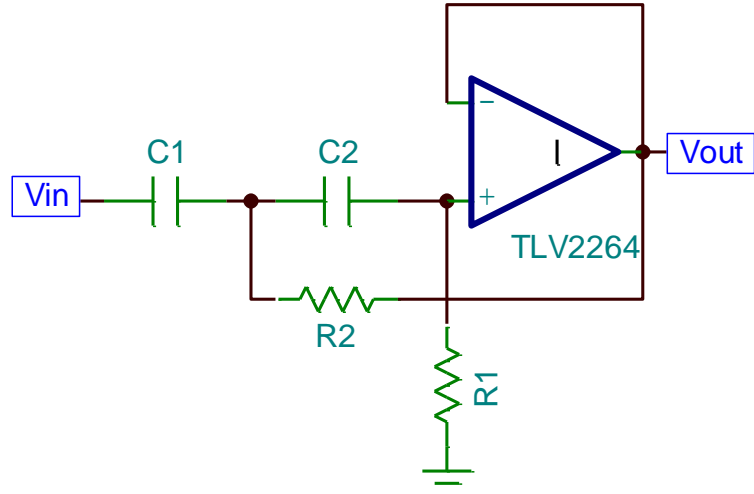


Figure 3.9. Sallen-Key Topology of Unity Gain High Pass Filter [16]

From figure 3.9, the transfer function of the High Pass filter is obtained by replacing the impedance values with the corresponding Laplace transforms i.e. R for the resistor and $1/sC$ for Capacitor in equation 3.5. Also to get rid of complex calculations, both the capacitors are assumed to have equal values.

$$A(s) = \frac{1}{1 + \frac{2}{\omega_c R_1 C} \cdot \frac{1}{s} + \frac{1}{\omega_c^2 R_1 R_2 C^2} \cdot \frac{1}{s^2}} \quad (3.13)$$

And the cut-off frequency, ω_c of the low pass filter is given by $\frac{1}{\sqrt{R_1 R_2 C_1 C_2}}$

By comparing the above equation with the generalized transfer function of the high pass filter, the filter coefficients and the gain are given by

$$A_\infty = 1 \quad (3.14)$$

$$a_i = \frac{2}{\omega_c R_1 C} \quad (3.15)$$

$$b_i = \frac{1}{\omega_c^2 R_1 R_2 C^2} \quad (3.16)$$

For the known filter type and desired cut-off frequency, the resistor values can be calculated for the given capacitor value as given by the following expressions.

$$R_1 = \frac{1}{\pi f_c C a_i}, R_2 = \frac{a_i}{4\pi f_c C b_i} \quad (3.17)$$

To obtain a filter with a flat frequency response and sharp transition region at 0.5Hz cut-off frequency, a 2nd order filter is sufficient for the desired performance after practicing with different implementations in the Pspice circuit simulation software. The final schematic obtained after meeting desired specifications for high pass filter is shown in figure 3.10 and respective components obtained from assumptions and equations 3.12 to 3.17 are furnished in table 3.2.

Table 3.2. High Pass Butterworth Filter Specifications

Spec.	Stage-1
1 st Order filter coefficient, a_i	1.4142
2 nd Order Filter Coefficient, b_i	1
Capacitors, C_1 & C_2	100 μ F
Resistor, R_1	4415.596 Ω (4.42K Ω)
Resistor, R_2	2207.755 Ω (2.21K Ω)
Quality Factor, Q_i	0.71
Frequency Ratio, K_i	1

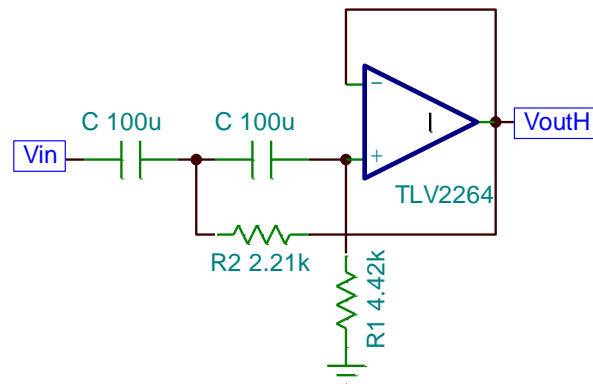


Figure 3.10. Designed 2nd Order High Pass Butterworth Filter

For implementation, standard resistor values of 1% tolerance, standard capacitor values of 20% tolerance and TLV2264 [14] operational amplifier are considered based on the feasibility. The simulated frequency response of the designed high pass filter is given in figure 3.11 with the zoomed region (inset) showing -3dB gain at 0.5Hz.

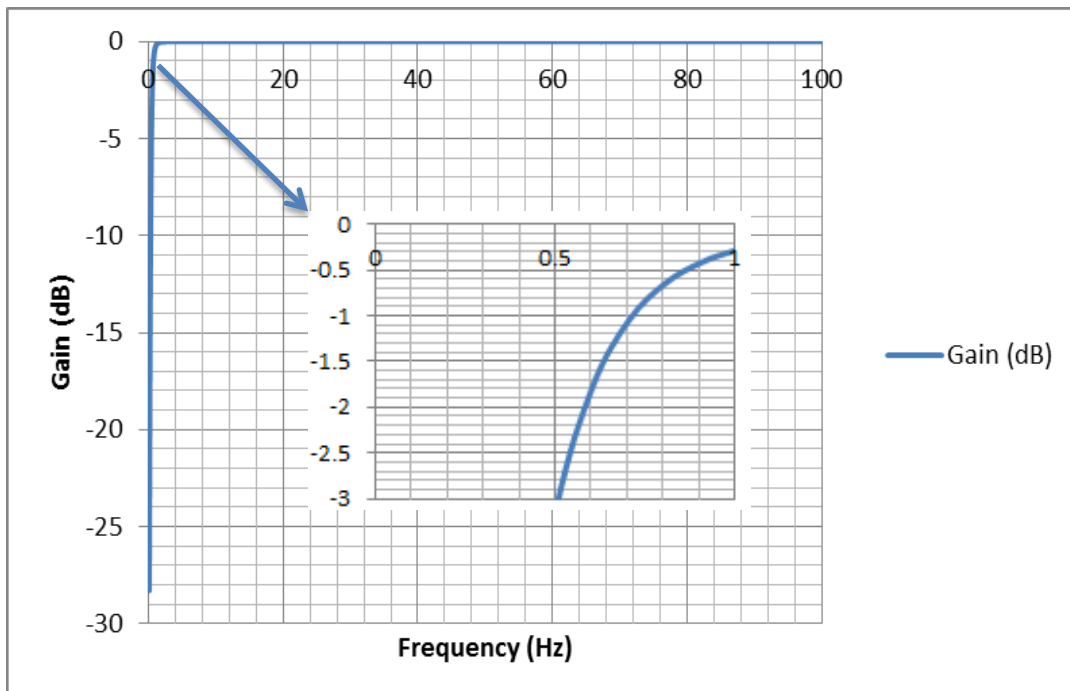


Figure 3.11. Simulated Frequency Response of Designed High Pass Filter on Pspice

3.4.3. Notch Filter

An Active 60Hz Notch filter is designed to filter the noise caused by the interference from the surrounding electrical lines. A twin-T topology [16] shown in figure 3.12 with the active feedback from the operational amplifier to increase the quality factor of the filter from 0.25 was implemented to obtain the band rejection at 60Hz.

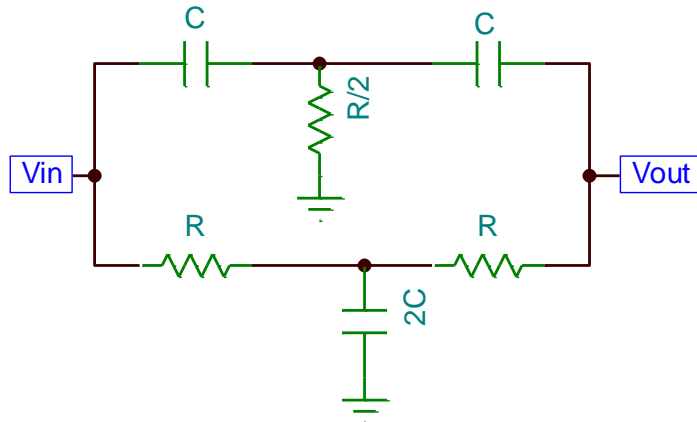


Figure 3.12. Twin-T Filter Topology for Notch Filter Design

The mid frequency of the twin T filter is given by $\frac{1}{2\pi RC}$. The output from the twin filter is fed into the active non-inverting filter to obtain the stable notch filter. The inner gain of the amplifier is $1 + \frac{R_1}{R_2}$. By assuming $C = 1\mu F$ and mid-frequency = 60Hz, the resistor (R) value obtained to be 2653.927Ω . Since there are no 1% standard resistors close to the obtained resistor value, two $1.33K\Omega$ resistors were connected in series. In order to compensate this resistor change, R_1 and R_2 are selected to be $1.96K\Omega$ and $2.00K\Omega$ respectively from multiple design implementations which are assumed to be equal initially to simplify calculations. The final schematic of this filter obtained from multiple implementations is shown in figure 3.13.

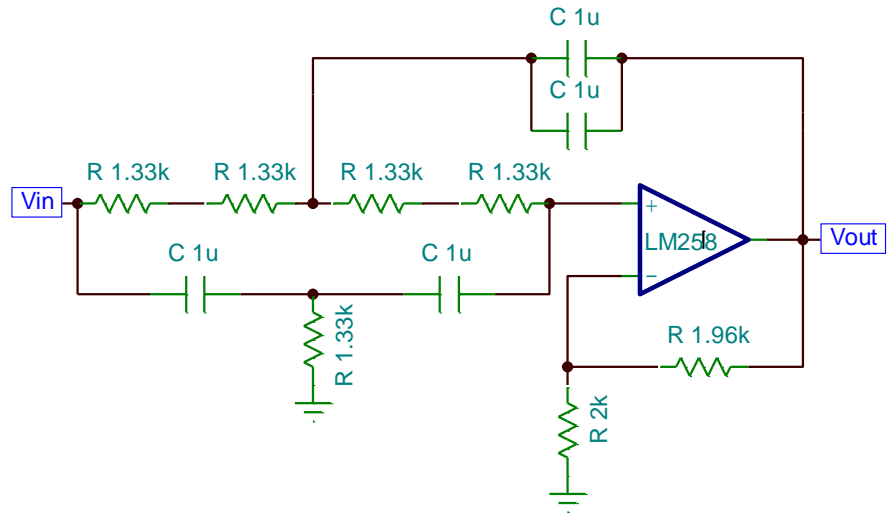


Figure 3.13. Schematic Diagram of Designed 60Hz Notch Filter

The gain of the designed notch filter is 1.98V/V or 5.93dB. Hence the overall gain from the amplifier and the filter becomes 9900V/V or 79.91dB. To implement this notch filter, an LM258 [15] operational amplifier is selected. The frequency response of the designed notch filter is given in figure 3.14 which shows large attenuation peak at 60Hz.

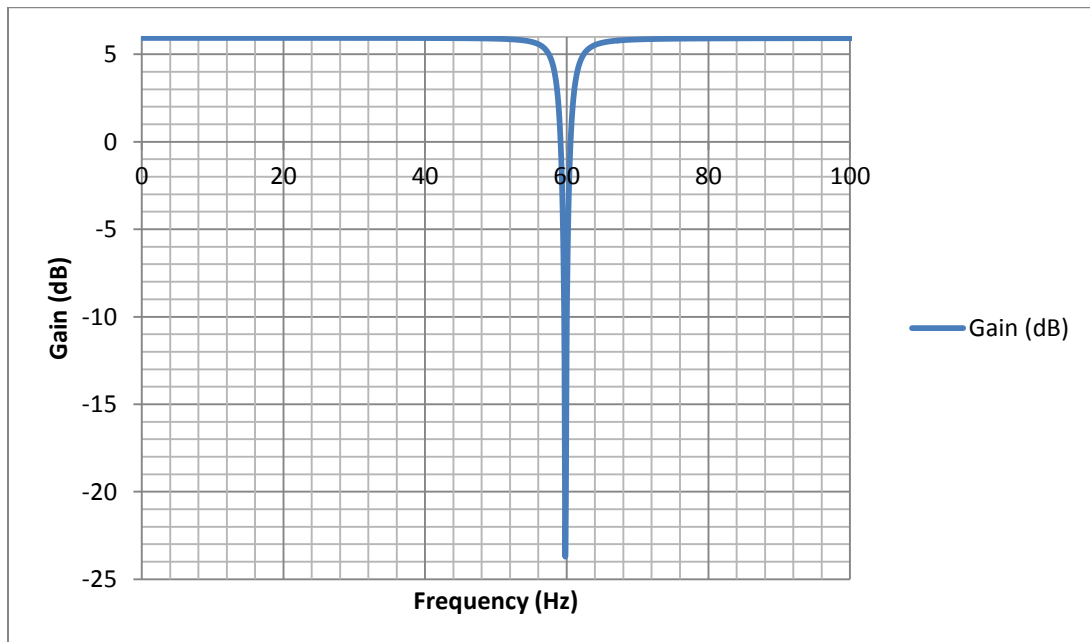


Figure 3.14. Simulated Frequency Response of Designed Notch Filter on Pspice

3.4.4. DC Bias Filter

A DC bias filter is needed before feeding the EEG signal into the micro controller for Analog to Digital conversion. Since the micro controller can only accept the positive voltage inputs up to a maximum of reference voltage selected on the ADC conversion. The maximum allowable internal reference voltage generator in the micro controller implemented in this project is 2.5V. Hence it is necessary to ensure that the signal varies in between 0V to 2.5V before A/D conversion.

The voltage range of the raw EEG signals is $\pm 100\mu\text{V}$ which will be amplified to $\pm 0.99\text{V}$ after notch filter stage. Hence a bias filter with an inverting gain of 0.5V/V and non-inverting gain of 1.25V DC is designed to bring the signal into the acceptable voltage range i.e. 0.75V to 1.75V . Hence the overall gain of the analog circuit is 5000V/V . The schematic of the DC bias filter to achieve the above specifications is shown in figure 3.15.

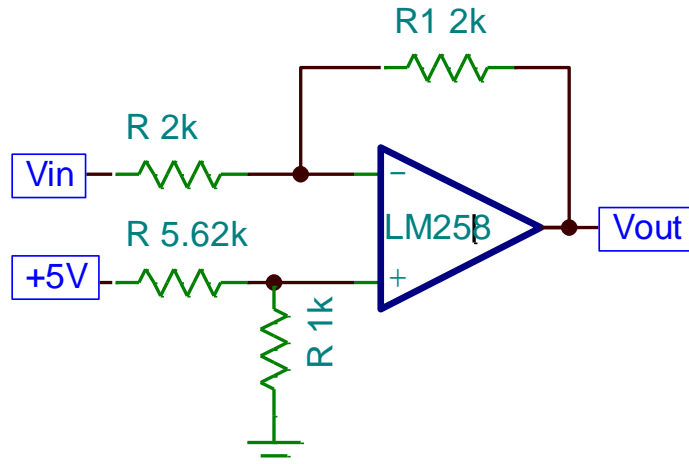


Figure 3.15. Schematic Diagram of Designed DC Bias Filter

The output voltage for the above design is given by

$$V_{out} = V_{in} \cdot \frac{-1.02K\Omega}{2.00K\Omega} + V^+ \cdot \left(\frac{1K\Omega}{6.62K\Omega} \right) \cdot \left(1 + \frac{1.02K\Omega}{2.00K\Omega} \right) \quad (3.18)$$

For the above equation the gain of input signal would be 0.5V/V with the addition of 1.25V from the power supply of +5V.

3.5. Power Management

This section describes the power supply design for amplifier integrated chips. As this project is designed and aimed to develop a portable instrumentation, the power supply range for operational amplifiers is selected to be in low voltage range which can be supplied by small batteries.

This project is designed to work on the voltage range of above 3 volts. Also there is a need to supply constant power supply to the operational amplifiers since the battery voltage is degraded with continuous usage. Hence a constant $\pm 5V$ power is supplied from a 9V battery using a voltage regulator. The voltage regulator circuit with the coupling capacitors is shown in figure 3.16.

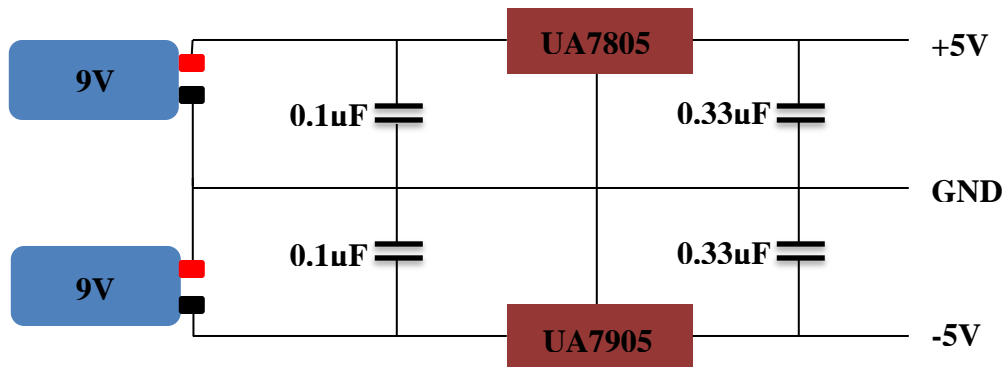


Figure 3.16. $\pm 5V$ Voltage Regulator Circuit to Power the Analog Circuit

From figure 3.16, two 9V Batteries are used to supply power to the circuit by connecting them in series. The positive terminal of one battery and negative terminal of another battery are connected together to form a zero voltage ground terminal. The bypass capacitors $0.1\mu\text{F}$ and $0.33\mu\text{F}$ are used on either side of the regulator to control the current fluctuations and supply clean DC power to the operational amplifiers. The 9V power supplies are regulated using positive 5V regulator UA7805 [17] and negative 5V regulator UA7905 [18] to provide a constant power supply voltage to the op-amp IC.

3.6. Digital Conversion and Data Transfer Design

From the analog circuit which includes design of the amplifier and an active filter (series of sub-filters in cascade structure), an analog signal with gain of 5000V/V which is free from known noise frequencies is obtained. This signal has to be digitized in order to transfer onto the analysis platform which is Android system in this design. To perform this operation an ultra-low power micro controller MSP430BT5190 [19] from Texas Instruments Inc. is used which is capable of Bluetooth operation when coupled with the CC2560 Bluetooth technology enabled PAN1323 [20] module from Panasonic Inc.

The MSP430BT5190 [19] microcontroller is employed to convert the input analog signal to digital signal using its 12-bit ADC module and transfer the converted data to PAN1323 Bluetooth module via Universal Serial Communications interface configured in Universal Asynchronous Receiver/Transfer (UART) mode. The PAN1323 module runs on the FreeRTOS operating system which works on the Bluetooth Serial Port Profile controlled by the microcontroller via UART interface.

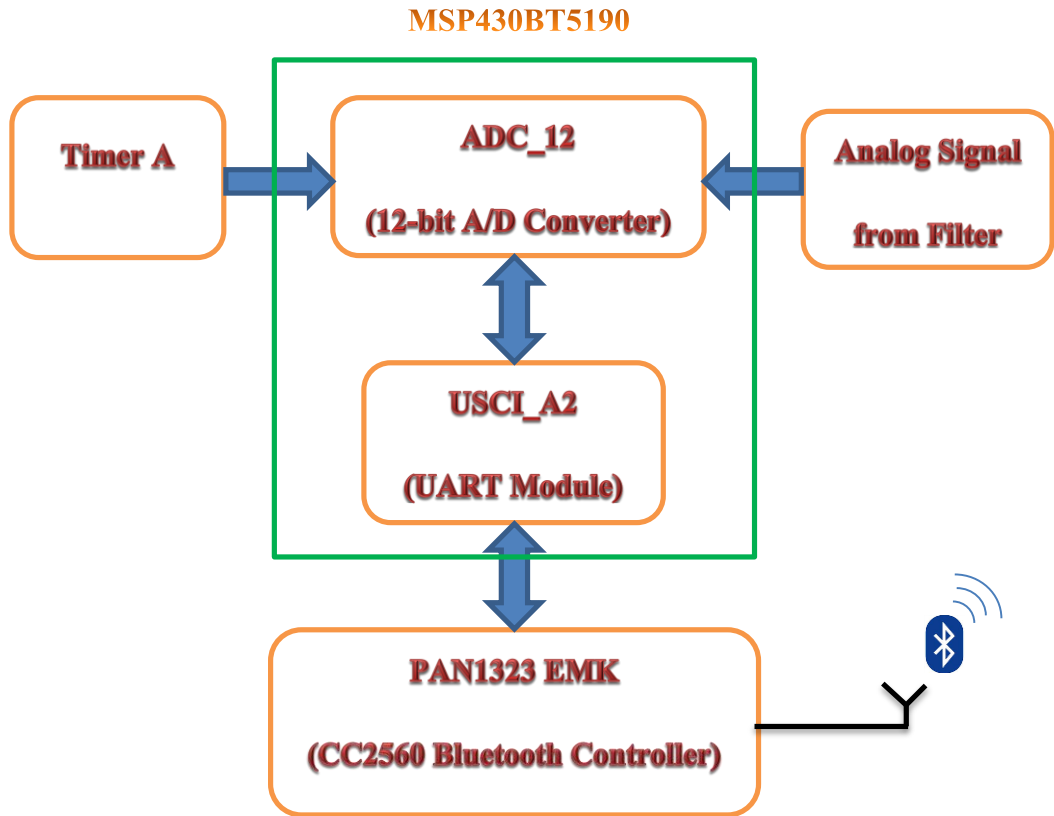


Figure 3.17. Block Diagram of System’s Digital Data Conversion and Data Transfer

Figure 3.17 shows the block diagram which indicates the data transfer from the MSP430BT5190 microcontroller to the PAN1323 Bluetooth controller which broadcast the signal to the surrounding Bluetooth devices. The microcontroller programming is done in C language using the IAR Embedded workbench software IDE from IAR systems and MSP430-CC2560 software development kit for MSP-EXP430F5438 from Texas Instruments Inc. which contains pre-defined templates for the Bluetooth operation on PAN1323 EMK kit [20]. To evaluate and implement this digital conversion and transfer, an evaluation board MSP-EXP430F5438 [21] is used to program the

MSP430BT5190 microcontroller using the USB debugging Interface MSP-FET430UIF [22] connected to the experimenter board via JTAG interface.

The Bluetooth operation is performed by the PAN1323 evolution module from Panasonic Inc. which is connected to the experimenter board via UART interface. The signal from the Bluetooth controller is transferred to the android mobile application by broadcasting on the 2.4MHz radio after a successful connection to the mobile device.

3.6.1 The Microcontroller - MSP430BT5190

The MSP430BT5190 [19] micro-controller is one of the devices in the MSP430 family of ultra-low power microcontrollers from Texas Instruments Inc. These microcontrollers are designed to have architecture compatible for low power mode operation to achieve the extended battery life for portable applications. It is a 16-bit microcontroller and configured with three 16-bit timers, high performance 12-bit analog to digital converter, up to four Universal Serial Communication Interfaces (USCI), real time clock module, Direct Memory Access (DMA) and 87 Input/output ports [19].

This microcontroller is specially designed for use with CC2560 Bluetooth core technology developed by the Texas Instruments Inc. incorporating Bluetooth Serial Port Profile which provides the wireless link that can be used in the portable instruments such as the bio-medical signal monitors.

3.6.1.1 Analog to Digital Conversion

The analog to digital conversion is carried out by the ADC_12 module [23] embedded in the MSP430BT5190 microcontroller and controlled by registers ADC12CTL0 and ADC12CTL1 and ADC12CTL2 [23]. The sampling rate of this analog

to digital conversion is 4.8 KHz and is configured using the above specified control registers. Also for this conversion the ADC module is configured to get the reference voltage of 2.5V which is generated internally by the module. Technically the lower (V_{R-}) and upper (V_{R+}) voltage limits of the input analog signal that can be converted into digital signal without errors are 0V and 2.5V. Hence a DC bias filter is used in the Active filter stage to ensure the signal amplitude is above 0V. The digital signal is calibrated by using the following expression: $N_{ADC} = 4095 \times \frac{V_{IN}-V_{R-}}{V_{R+}-V_{R-}}$.

Where, V_{IN} = Input Analog Voltage.

The data from the ADC module is stored in the temporary register ADC12MEMx which is configured in the ADC12MCTLx register along with the input port and the reference voltage selector. This data conversion is driven by the ADC interrupt vector which creates interrupt after each successful conversion. The converted data will be accessed by the UART module when it needed to send data to the PAN1323 module for broadcasting the signal via Bluetooth radio.

3.6.1.2. Universal Asynchronous Receiver/Transfer (UART) mode Transmission

UART is the Universal Asynchronous Receive/Transfer mode of communication in the embedded hardware platforms. It can be used to send the data bytes either in serial or in parallel connection by transmitting the data in 8-character data frames by appending start and stop bits on either side whenever the controller is ready for data communication and hence the name asynchronous transmission.

The UART transmission is carried by the Universal Serial Communication Interface (USCI) module [23] embedded in the MSP430BT5190 microcontroller by

appropriately configuring the control registers administering the functionality of USCI module. The signal routing between both controllers for UART transmission is shown in figure 3.18 which also indicates the port configuration used in this work.

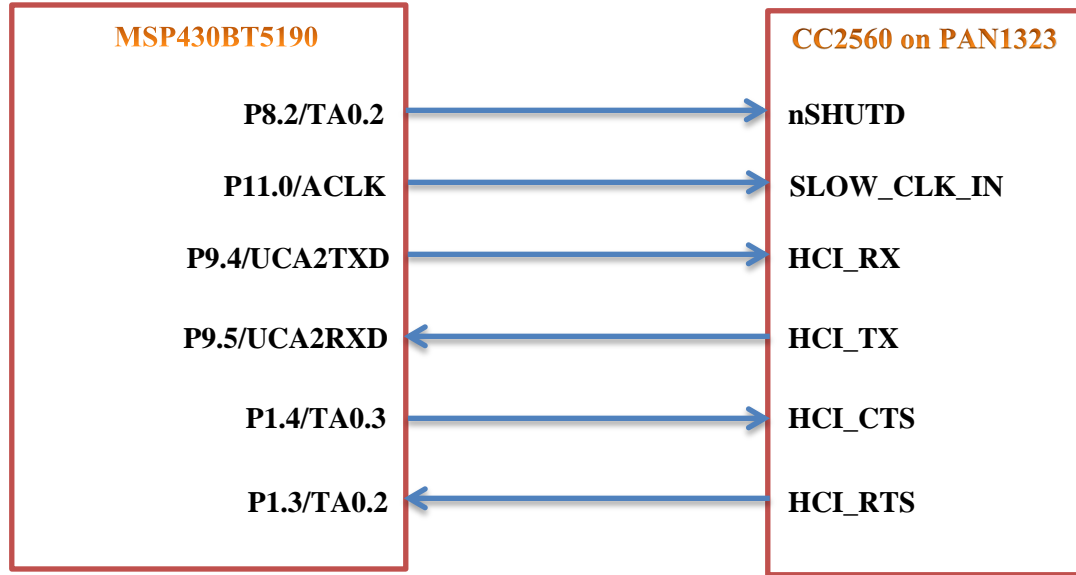


Figure 3.18. Hardware Connections for UART Transmission between MSP430BT5190 and CC2560

The UART is configured to access the ADC conversion result from ADC12MEMx registers and also from other registers (such as where the instructions for the Bluetooth operation are stored) and transmit them to the controller (PAN1323EMK) whenever requested.

The UART operation is operated and configured using the control registers of the Universal Serial Communication Interface (USCI) [23]. UCAXCTL0 and UCAXCTL1 are the registers used to configure USCI to operate in UART mode and selection of transmit parameters such as the character length, clock source, type of data and error controls. UCAXBR0 and UCAXBR1 are the baud rate registers used to set the baud rate

of the USCI module and 115200 baud rate is used in this project. UCAxTXBUF and UCAxRXBUF are the data shift registers for transmission and reception respectively to transmit the data to the Bluetooth data.

3.6.2 CC2560 Bluetooth Operation

The Bluetooth operation is performed by the PAN1323EMK [20] kit from Panasonic Inc. which uses the CC2560 Bluetooth core technology from Texas Instruments Inc. PAN1323 runs on a FreeRTOS operating system which is loaded onto it by the microcontroller. The block diagram of CC2560 chip on PAN1323 board is shown in figure 3.19 which indicates the control/data signals transmission and transceiver system for Bluetooth communication.

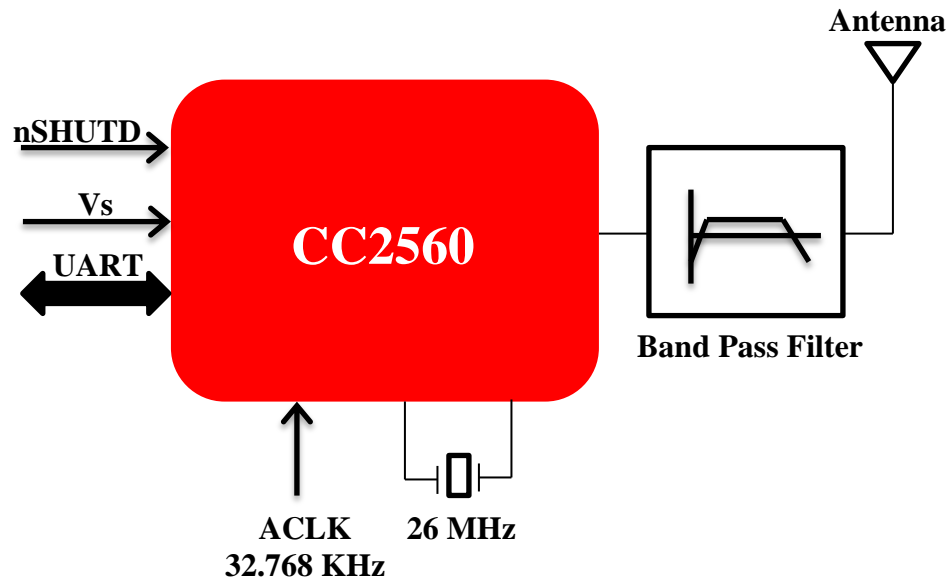


Figure 3.19. Block Diagram of CC2560 Chip [20]

The controls and initialization parameters required for this Bluetooth operation are programmed using the MSP430-CC2560 Software Development kit [27]. This kit

contains the template program and the header files needed for the CC2560 Bluetooth core operation which runs on the FreeRTOS operating system. The Application Programmers Interfaces (APIs) [27] required for Bluetooth initialization, data transmission and connection parameters are defined in EtherMind Bluetooth Serial Port Profile (SPP) [27] which implements the Bluetooth stack layer shown in figure 3.20.

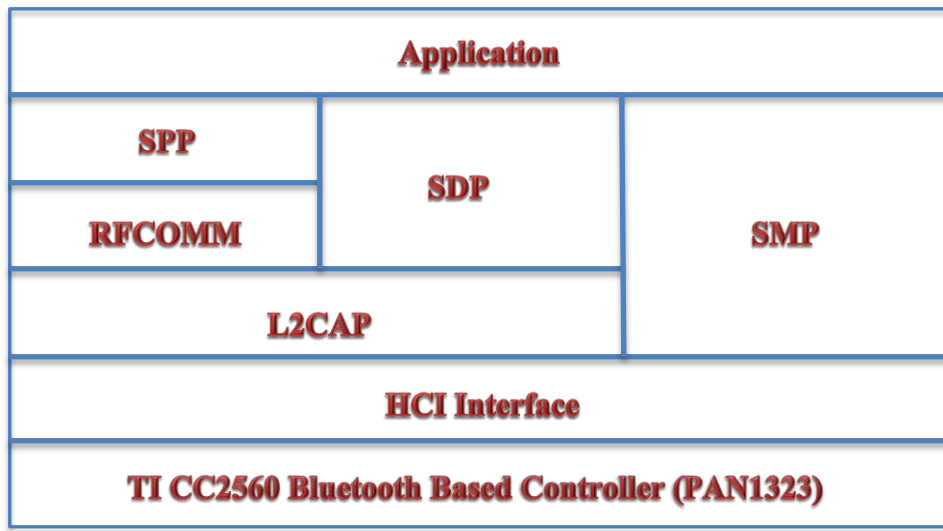


Figure 3.20. EtherMind Bluetooth Serial Port Profile Stack Layer

The HCI Interface and its above layers in the Bluetooth SPP protocol are implemented on host microcontroller which is MSP430BT5190. From figure 3.20, ‘Application’ is the layer which receives and sends the data into the software. ‘SPP’ is the Serial Port Profile layer used to read and write data between the application layer and HCI layer. It is used to rearrange the data so as to facilitate the serial communication via Host Controller Interface. ‘RFCOMM’ is the Radio Frequency communication layer that provides the RS-232 standard for serial port communication to the device. ‘SDP’ is the Service Discovery Protocol later used to discover and exchange Bluetooth profiles assigned with identifiers with the other Bluetooth devices. ‘SMP’ is the Security Manager

Protocol used for the authenticating devices if device pairing is implemented. ‘L2CAP’ is the Logical Link Control and Adaption Protocol layer used to multiplex and arrange the data packets between the physical layer (Host Controller Interface and lower layers) and the higher layer protocols. ‘HCI Interface’ is the Host Controller Interface layer which is the communication interface between the host controller and the Bluetooth controller IC i.e. UART Interface in this system design. It is used to transfer the commands, events and the data packets to the Bluetooth IC. The last layer is the Bluetooth IC which is PAN1323 in this system design and is connected to the microcontroller via UART interface.

3.7. Android Application

The data that is transmitted from the PAN1323 Bluetooth controller via Bluetooth radio will be received by the android operated mobile phone. To facilitate the data reception on the phone, an android application that can communicate with the Bluetooth hardware of the phone has to be installed in the mobile system. For this purpose, the sample project from the android SDK named “Bluetooth Chat” [25] and various other sample applications [24] which can display the real time data are studied.

The Bluetooth chat application [25] contains the Java programs related to the Bluetooth operation and connectivity of the data with the other devices. The waveform application [24] contains the Java programs related to the graphical layout which can display the plotted data as it acquires from the Bluetooth hardware. The above said Java programs are collectively inherited into the development of this application. The flow chart related to the development and functioning of Android Application is given in figure 3.21.

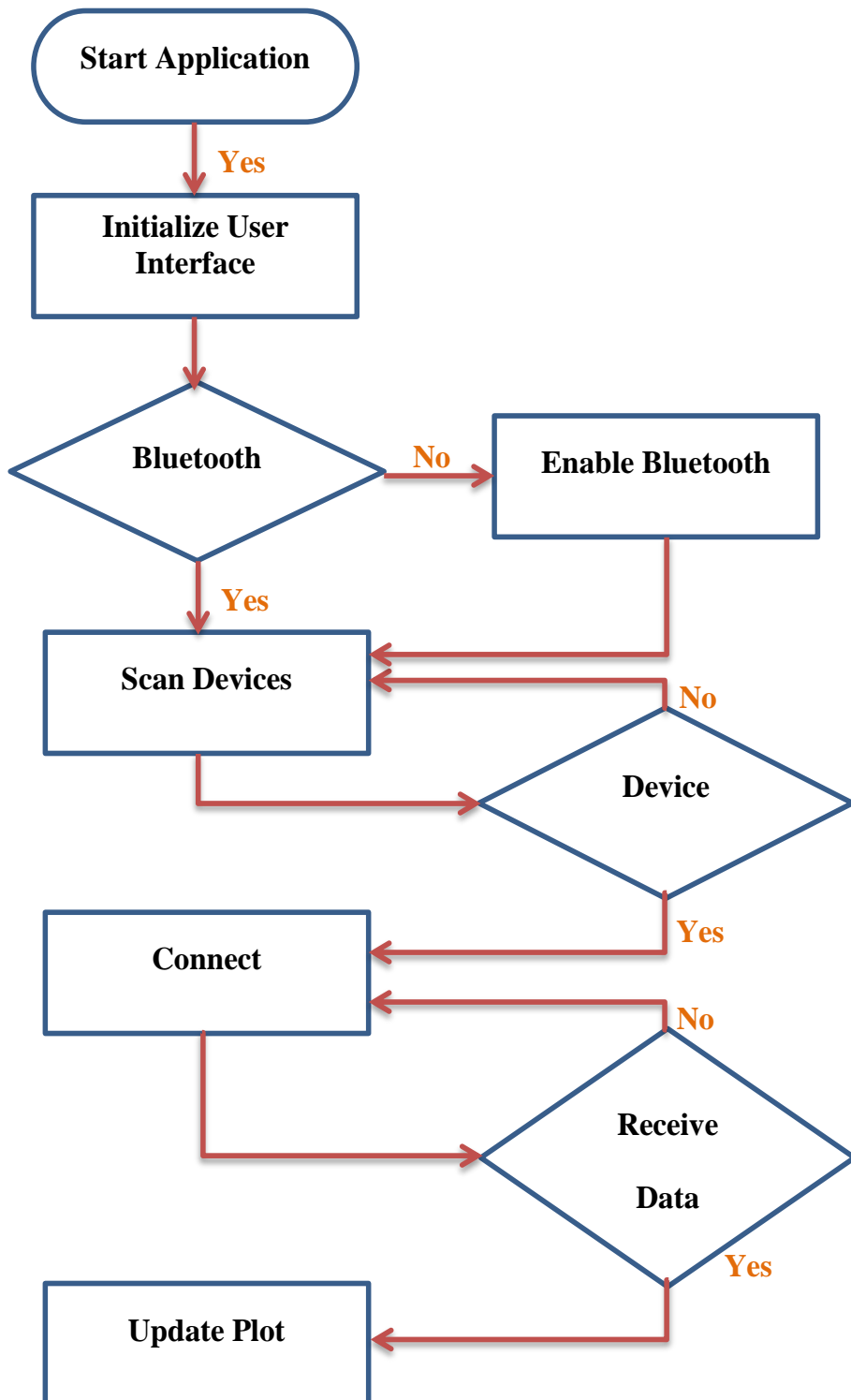


Figure 3.21. Flowchart for Data Reception using Bluetooth on Android Mobile

This Android application is developed using the Android software development kit which contains the java files that perform the algorithm to acquire data and plot it in real time. Once the application is started, all the parameters in the graphical user interface are initialized to the default values. The application checks for the Bluetooth compatibility and availability of the devices. The data communication is routed through the RF Communication channel over the Host controller Interface of the Bluetooth hardware of the android device. The application is allowed to receive the data after successful connection to a device and the plot is updated in real time.

3.8. Summary

So far the design procedure for the implementation of the prototype EEG signal acquisition system is presented in this chapter. The analog circuit has been designed to amplify the raw EEG signals collected from the electrodes and filter the amplified signal for the known sources of noise. After preprocessing, the analog signal is digitized using MSP430BT5190 microcontroller and transmitted to the PAN1323 Bluetooth controller for the data transmission onto an Android operated mobile via Bluetooth radio. A special software application is designed to receive and display the signal on Android mobile.

CHAPTER – IV

SYSTEM'S REALIZATION, PARAMETERS AND RESULTS

4.1. Analog Circuit Realization on a PCB

The analog circuit design consists of the implementation of amplifier and filters designed in chapter III. A Printed circuit board layout is designed to realize the physical connections between the components which are hand soldered on the board. The PCB is designed using the “PCB Artist” software package from the Advanced Circuits Inc. This software package is able to convert the schematic diagram to PCB layout which is compatible with the given constraints. The constraints and parameters for the PCB design are given in the table 4.1.

Table 4.1. PCB Design Constraints for Analog Circuit

Parameter	Value
Material Type	FR4
No. of Layers	2
Material Thickness	0.062 Inches
Copper weight	1 Oz
Min. Track width	0.010 Inches
Min. Track Gap (Routing)	0.015 Inches
Min. Via hole	0.015 Inches

The foot prints for the components used in the PCB layout design are designed manually in the PCB part creator package from Advanced Electronics Inc. using the data

sheets of the respective components. The PCB layout design for the analog circuitry is shown in figure 4.1.

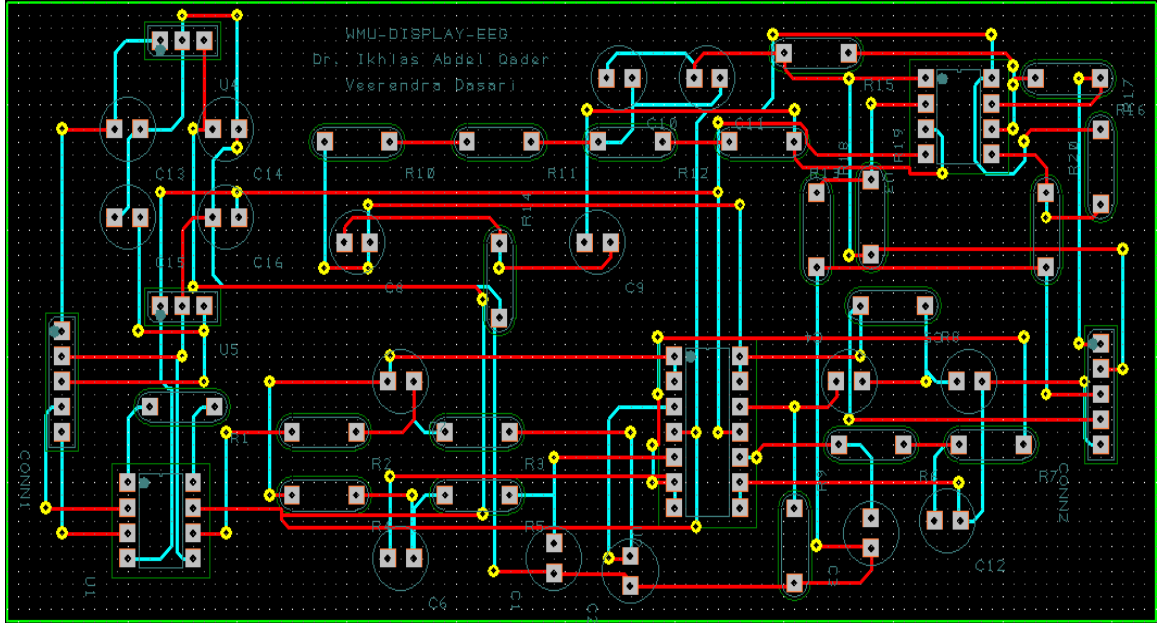


Figure 4.1. PCB Layout Design of Analog Circuit

For the PCB layout design, the foot prints which indicate the dimensions of the components and its parts have to be known. The data sheets of the components used in the design are studied to create the parts and its layouts using the Parts creation tutorial in the PCB Artist software. Once these parts are created, these are used to design the PCB layout for the Analog circuits discussed in the previous chapter. After receiving the PCB from manufacturing, the components are inserted and soldered manually. The PCB with the analog circuit is shown in the figure 4.2.

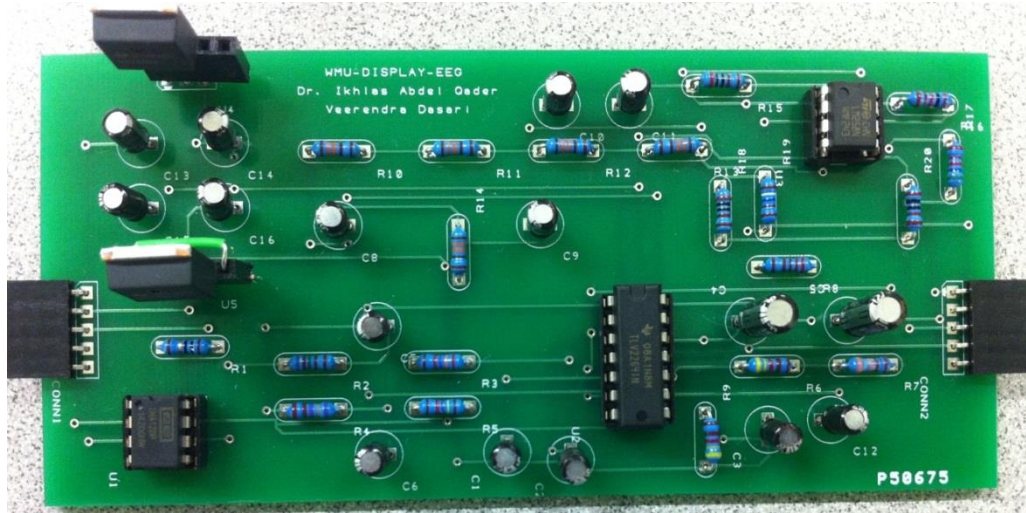


Figure 4.2. Printed Circuit Board of Analog Design proposed in Chapter - III

In the PCB in figure 4.2, it accommodates the circuits designed in the previous chapter i.e. $\pm 5V$ Input Voltage Regulator, Amplifier, Low Pass Filter, High Pass Filter, 60Hz Notch Filter, DC Bias Filter. A 5-pin connector is used on either side of the board to facilitate input and output connections which includes the battery connection, input EEG signal, output signal from different stages of the circuit.

4.2. Gain and Frequency Response of the Analog Circuitry

Due to the non-availability of generator that can generate the ultra-low voltage signals, the gain and frequency response of the different stages of the analog circuit is tested with the sample ultra-low voltage signal generated from the voltage divider circuit. A sinusoidal signal of 1V amplitude from the waveform generator is given as an input to the circuit with $1.007M\Omega$ and 99.5Ω in series and the voltage output across the 99.5Ω resistor is given as an input to the PCB. The laboratory setup for this testing is shown in figure 4.3.

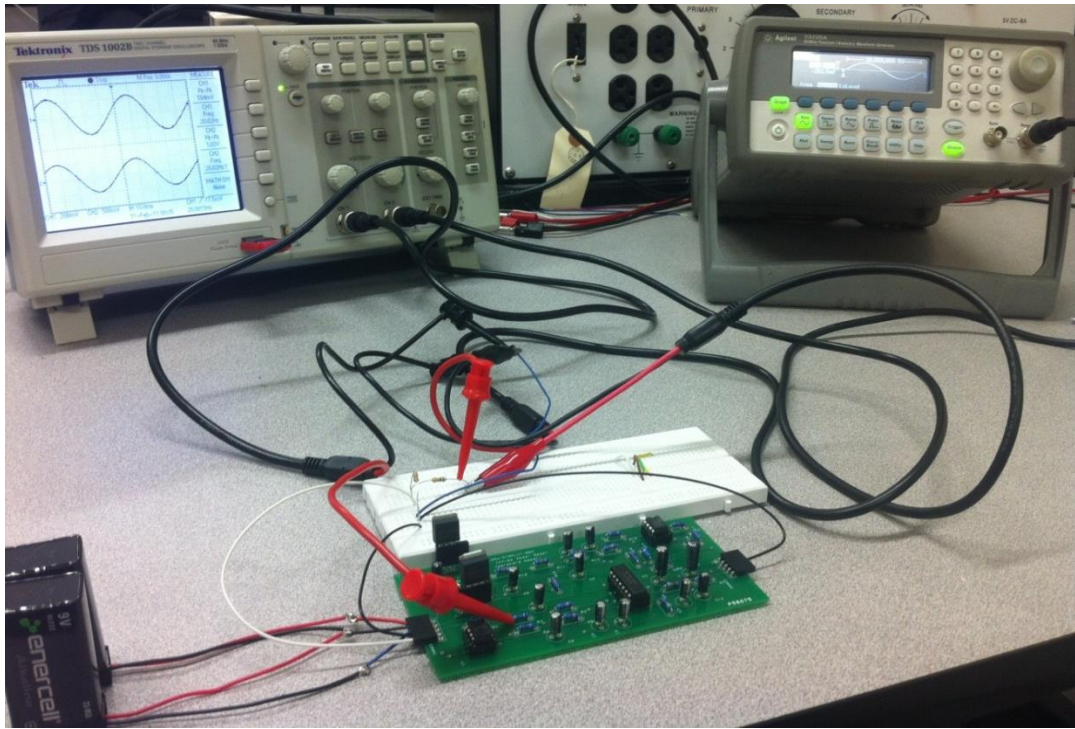


Figure 4.3. Laboratory Setup to Test Different Stages in Analog Circuit

Due to unavailability of the instrument that can measure the ultra-low voltage signals, the amplitude of the sample signal given as an input to the amplifier is manually calculated to be:

$$V_{in}^+ = 1.02V \times \frac{99.5\Omega}{1.007M\Omega + 99.5\Omega} = 100.75\mu V_{pp} \quad (4.1)$$

4.2.1. Amplifier

The amplitude of the voltage output from the INA128 amplifier is found out to be 496mV_{pp}. Hence the experimental gain of the amplifier is found out to be 4923.08V/V or 73.84dB. The oscilloscope screenshot for the amplifier stage is shown in figure 4.4 from which the gain of the amplifier stage at 10Hz is obtained.

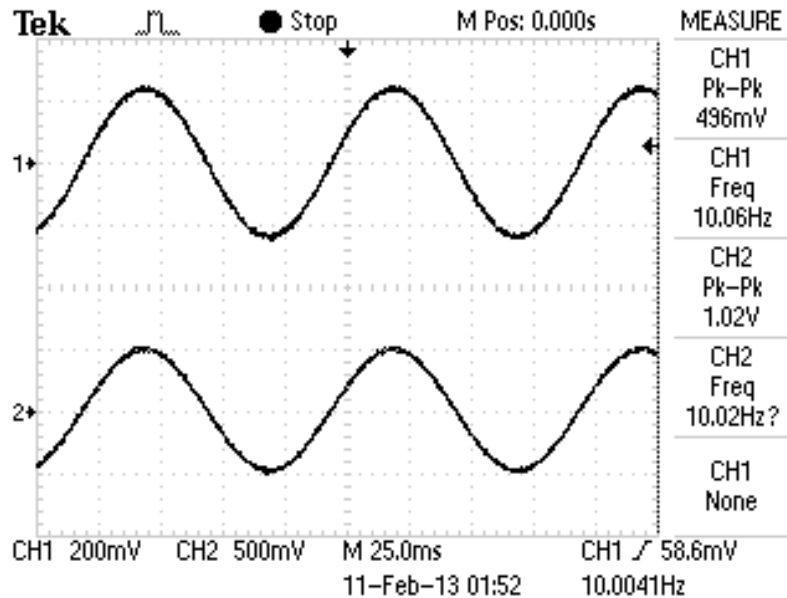


Figure 4.4. Oscilloscope Screenshot for Amplifier Output Signal at 10Hz.

From figure 4.4, the channel 1 represents the output signal from the amplifier and the channel 2 represents the signal fed into the voltage divider circuit. The measurement menu indicates the corresponding voltages and frequencies of channels.

4.2.2. Low Pass Filter

The frequency response of the Low pass filter is computed by recording the amplitudes of the both input and output signals using the dual channel oscilloscope by varying the frequency of the input signal in uniform steps. The gain of this filter is plotted with respect to the frequency as shown in the figure 4.5.

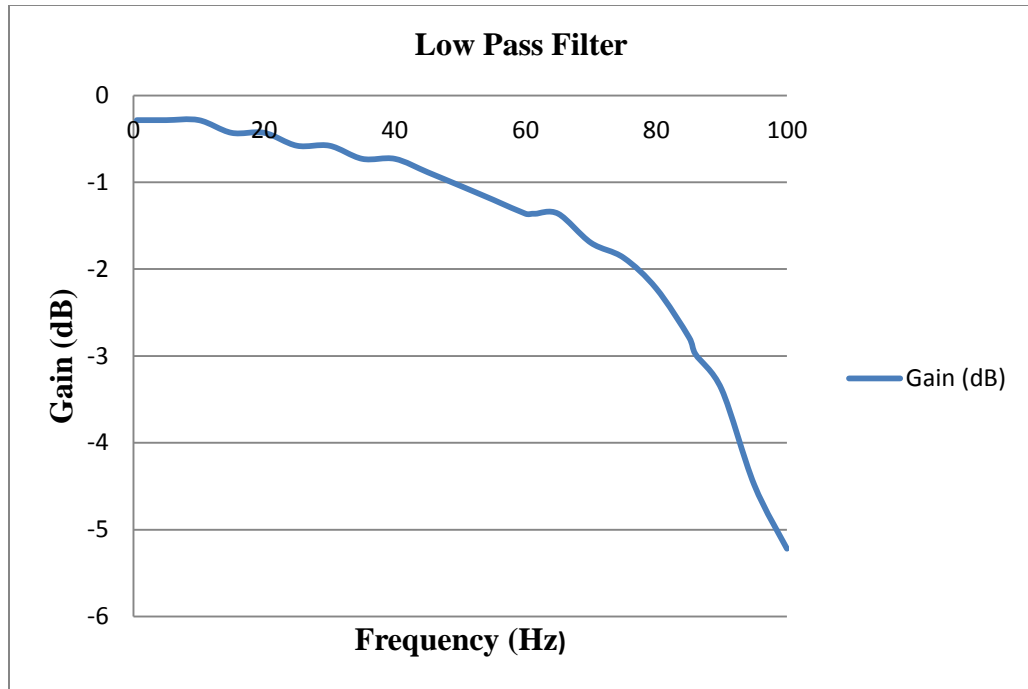


Figure 4.5. Frequency Response of Implemented Low Pass Filter ($f_c = 100\text{Hz}$).

The Low pass filter is designed to have the cutoff frequency (i.e. -3dB frequency) of 100Hz. But from figure 4.5 during the implementation, the cutoff frequency is observed at 87Hz. The reason for the shift in the cutoff frequency is due to the difference in the actual values of the components to the designed values due to the implementation of 3 stage analog low pass filter with the 1% tolerant through-hole resistors and 20% tolerant capacitors.

4.2.3. High Pass Filter

The frequency response of the high pass filter is computed in the similar manner to that of low pass filter. The gain of this filter is plotted with respect to the frequency in shown in figure 4.6 which also indicates the gain at cutoff frequency in zoomed region (inset) on the plot. The ripples in the plot are due to the imperfections in the voltage

collection using the function generator and oscilloscope and are not related to the functionality of filter.

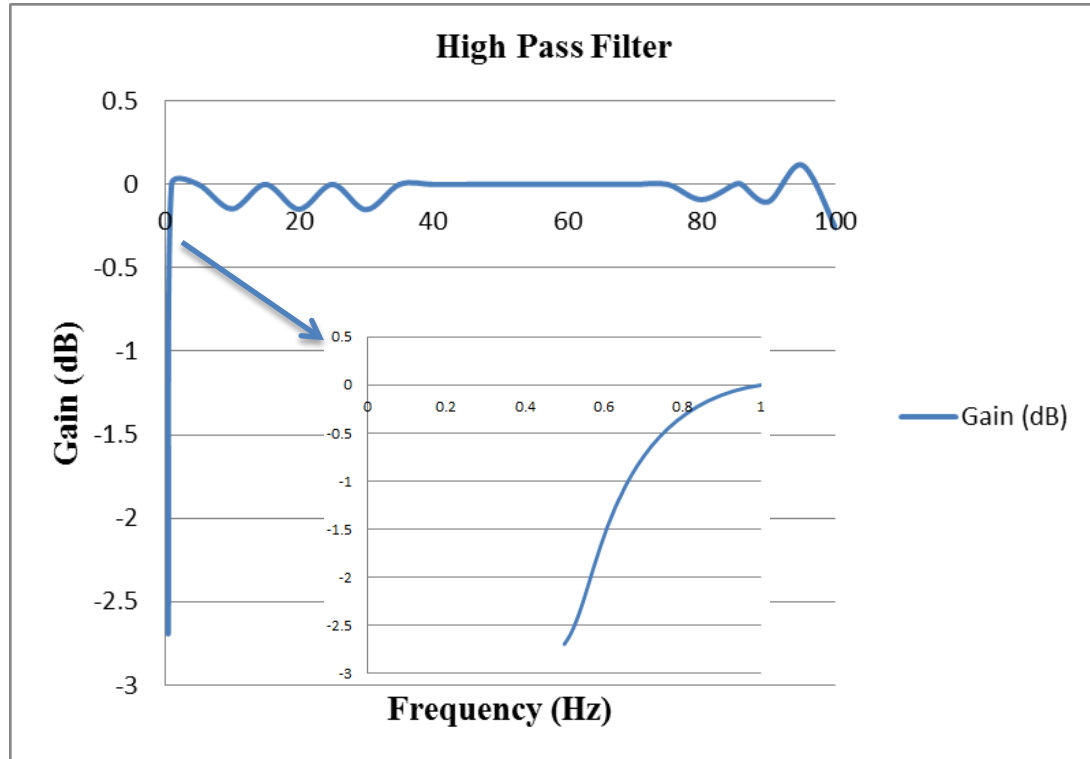


Figure 4.6. Frequency Response of Implemented High Pass Filter ($f_c = 0.5\text{Hz}$).

The High pass filter is designed to have the cutoff frequency (i.e. -3dB frequency) of 0.5Hz. And from figure 4.6 during the implementation, the cutoff frequency is observed at 0.5Hz. This is a single state implementation of the high pass filter. Unfortunately the function generator and the oscilloscope are not very accurate to measure the signal at the frequencies below 1Hz. And hence the close approximation is estimated based on the recordings.

4.2.4. 60Hz Notch Filter

The frequency response of the notch filter is computed by recording the amplitudes of the output of the high pass filter (since output of high pass filter is the input of the notch filter) and the output of the notch filter from the dual channel oscilloscope. The gain of the notch filter is observed to be 2V/V or 6dB. A frequency response of the actual filter is shown in figure 4.7 which indicates an attenuation peak at 61Hz.

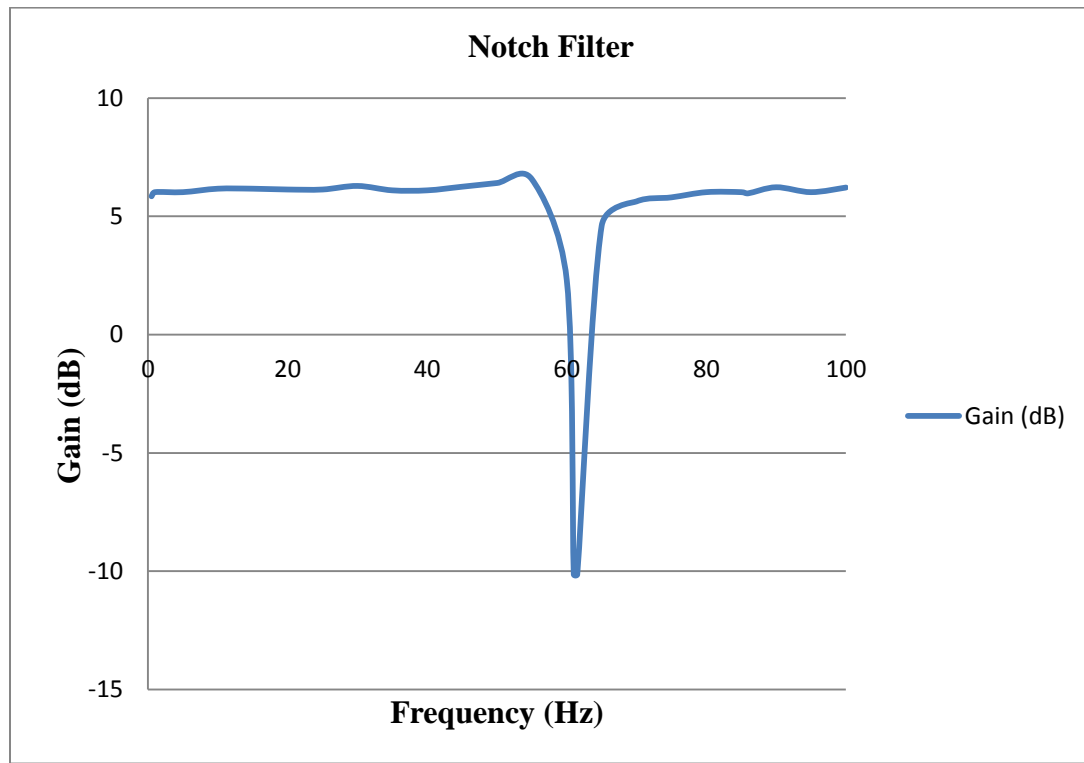


Figure 4.7. Frequency Response of Implemented 60Hz Notch Filter.

From figure 4.7, the implemented notch filter rejects the frequencies between 60Hz and 63Hz which is obtained from the above mentioned testing.

4.2.5. DC Bias Filter

This filter is designed to add 1.25V DC voltage to the output so as to bring the signal to have the positive range between 0V to 2.5V. This actual filter implemented here in the design attenuates the input signal by 0.5V/V with the addition of 1.13V DC to the signal so as to bring the gain of the filter stage to Unity. The figure 4.8 show the DC voltage added to the input signal by the measurement parameter ‘Mean’ on channel 1 which is 1.13V.

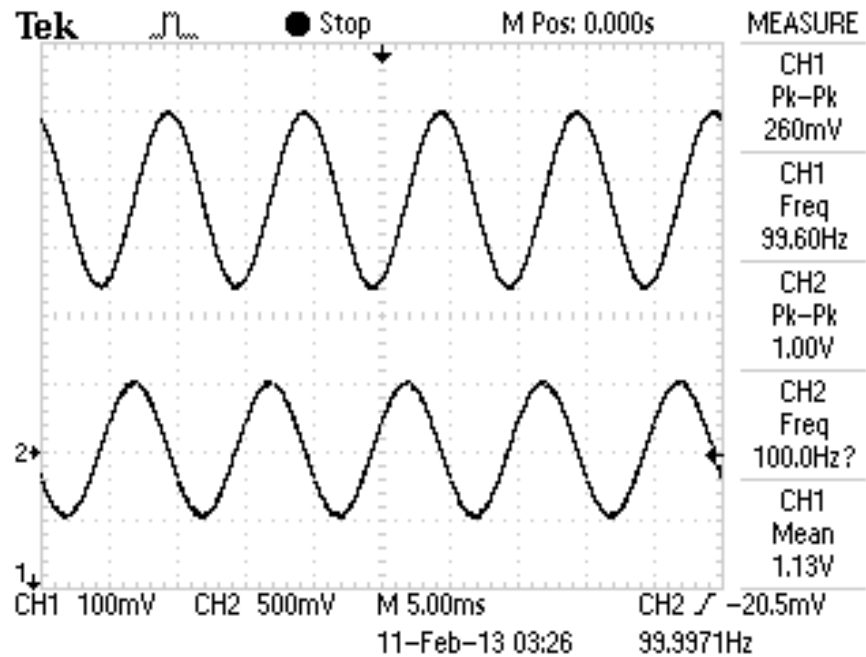


Figure 4.8. Oscilloscope Output of DC Bias Filter indicating Mean Voltage of Signal

In the figure 4.8 channel 1 is the output signal from the DC Bias filter and channel 2 is the input provided to the voltage divider circuit at 100Hz. The gain of the DC Bias filter stage is computed by recording the voltages using the dual channel oscilloscope on either sides of the filter at different frequencies in uniform steps. The gain obtained has a mean value of around 0.49V/V or -6.2dB which can be observed in figure 4.9. This

uncertainty in the gain is due to the change in the DC offset and also due to the inconsistent recordings from the measuring instruments. The frequency response of the DC Bias filter is shown in figure 4.9 and the ripples are due to discrepancies in the recording schemes.

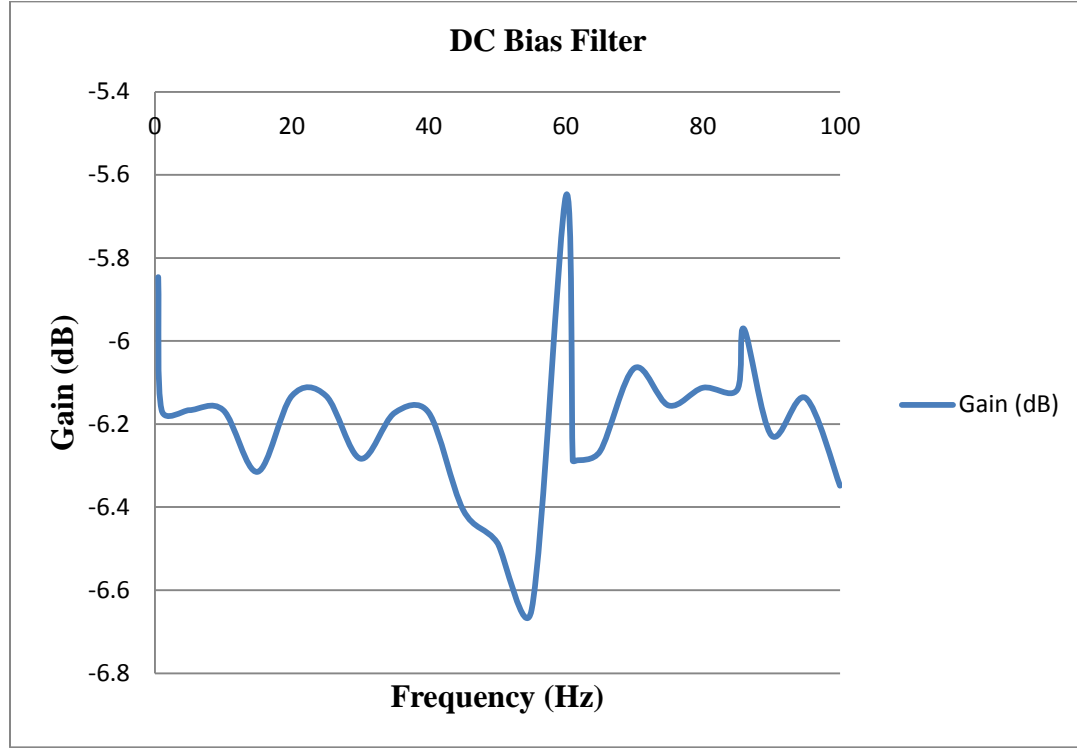


Figure 4.9. Frequency Response of Implemented DC Bias Filter

4.2.6. Frequency Response of Analog Filter Circuit

The figure 4.10 depicts the combined frequency response of the filter circuits when a sample signal is given as an input to the amplifier with amplitude of $100\mu\text{V}$ generated by the voltage divider circuit. Due to the non-availability of the spectrum analyzer, the accuracy of this frequency response which is calculated point to point is not consistent.

For the analog circuitry on the printed circuit board, frequencies at which the gain is -3dB are found out to be 0.5Hz, 59Hz, 65Hz, 87Hz i.e. the frequencies other than 0.5Hz to 59Hz and 65Hz to 87Hz for which the gain is below -3dB are rejected through the filter which are obtained from the figure 4.10.

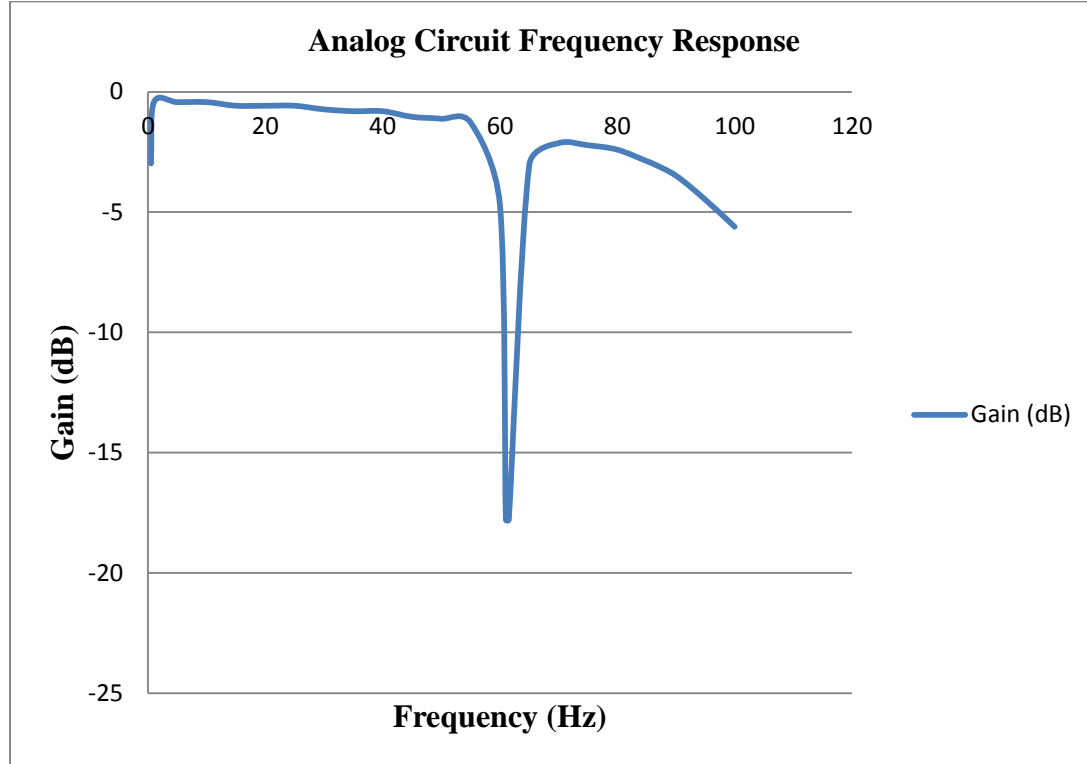


Figure 4.10. Frequency Response of Implemented Analog Circuitry on PCB

The frequency response obtained in the real time implementation is close to the designed circuit. As the circuit is designed to allow the low frequencies, a small change in the component values will result change in the cutoff frequencies.

Due to the presence of the capacitors in the circuit there is delay in the signal i.e. the phase difference between the input signal to the PC board and its output signal at a frequency of 20Hz is found out to be 115.2 Degrees or 16ms time delay as shown in

figure 4.11. This delay varies with the frequency. Also for this real time application, the delay is desired to be low.

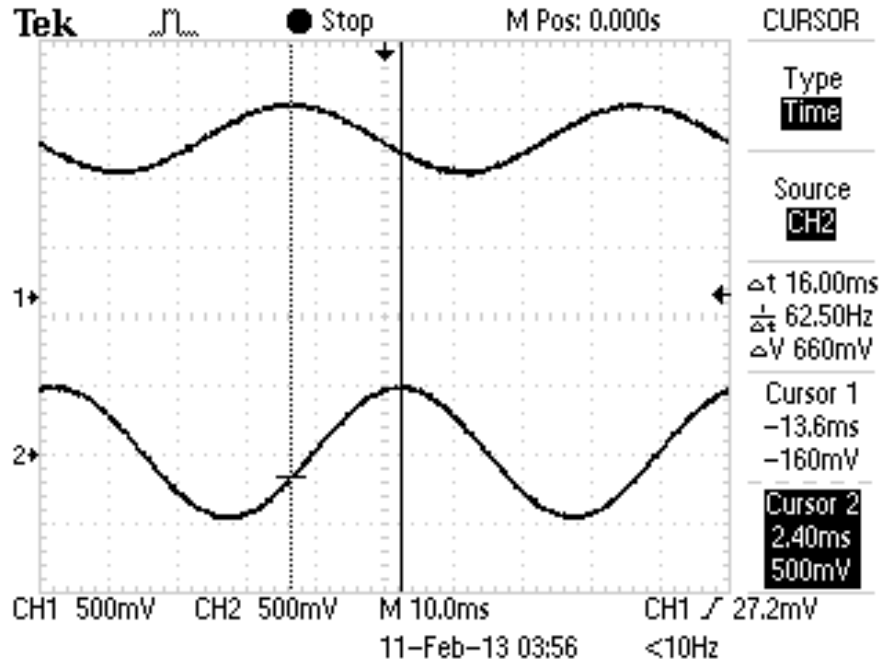


Figure 4.11. Phase Difference (Time Delay) between the Input and Output Signals for Analog Circuit at 20Hz.

4.2.7. Comparison between Design and Implementations

The parameters that are obtained from the implemented analog circuitry are compared with the designed values for quality and reliability of the circuit for signal preconditioning and are furnished in the table 4.2 and figure 4.12 indicates the comparison between the simulated and obtained frequency response of the analog circuitry.

Table 4.2. Parameter Matching between the Designed and Implemented Circuits

Parameter	Design	Implementation
Amplifier Gain	5000 V/V or 74dB	4923.08 V/V or 73.84dB
Low Pass cutoff frequency	100 Hz	87 Hz
High Pass cutoff frequency	0.5 Hz	0.5 Hz
High attenuation notch frequency	59.8 Hz	61.5 Hz
Notch Filter Gain	2 V/V or 6dB	2 V/V or 6dB
DC Bias voltage	1.25V	1.13V
DC Bias Filter Gain	0.5 V/V -6dB	0.49 V/V or -6.2dB
Active filter gain	~0dB	-1dB to -3dB

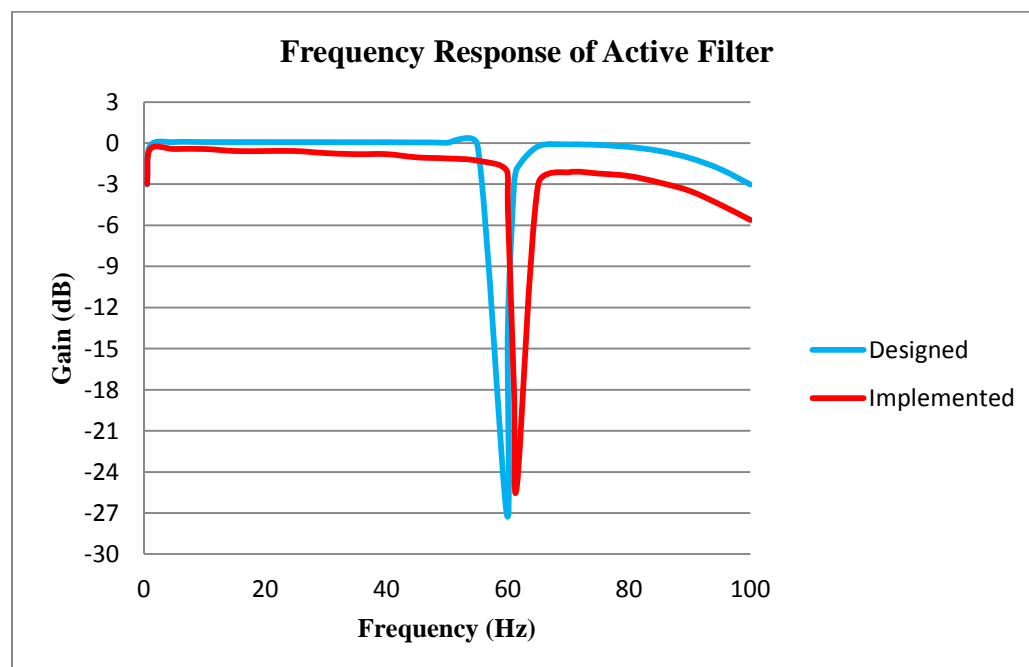


Figure 4.12. Frequency Response Comparison to the Designed and Implemented Circuits

4.3. Digital Circuit Realization on MSP-EXP430F5438 CC2560 Evaluation Platform

4.3.1. Hardware Connections

The digital circuit converts the signal from the analog circuit into the digital signal and transmits to the Bluetooth controller which in turn transmits the signal via Bluetooth wireless protocol. The two major parts of this circuit are the MSP430BT5190 microcontroller and the CC2560 Bluetooth controller. These two chips are connected via Universal Serial Communication Interface and data is transmitted in Universal Asynchronous Receive / Transfer mode.

To implement this circuit, the evaluation platform on MSP-EXP430F5438 Experimenter board coupled with PAN1323 Evolution module kit is used. The MSP-EXP430F5438 Experimenter board which is shown in figure 4.13 is used to initialize and program the microcontroller and PAN1323 module which is shown in figure 4.14 incorporates the CC2560 Bluetooth core technology for Bluetooth operation.

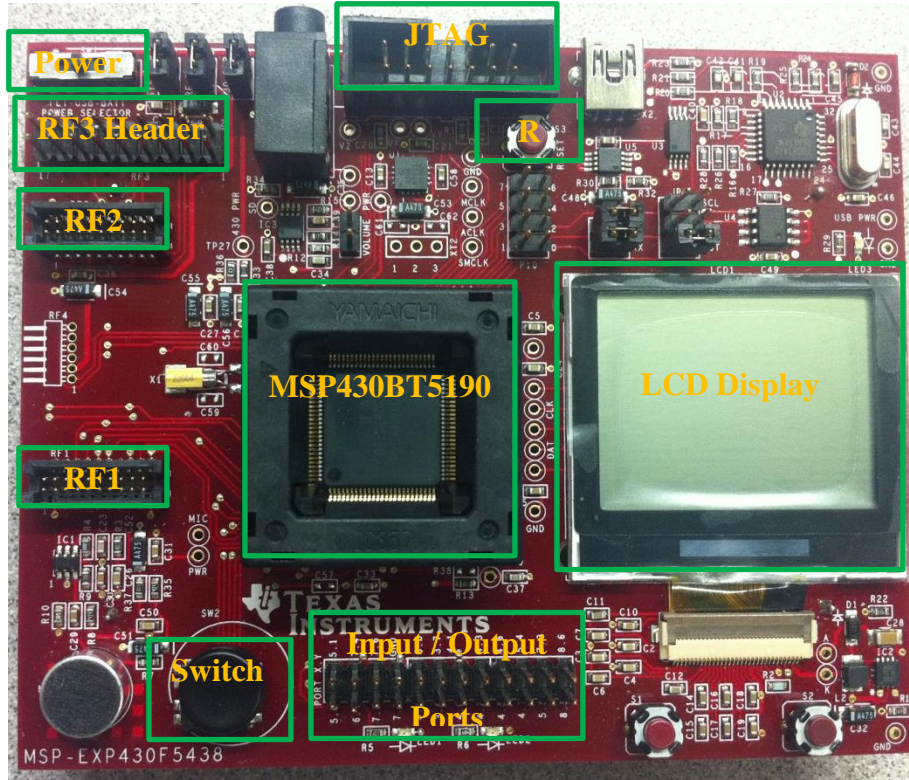


Figure 4.13. MSP-EXP430F5438 Experimenter Board

In figure 4.13, Power is used to select the source of power supply which can be anyone from JTAG interface, USB interface and BATTERY connected to the back of the board. ‘JTAG’ is the interface used to connect the experimenter board with the computer to debug and transfer the program via the MSP-FET430UIF USB debugging interface. “Input / Output Ports” is the interface used to transmit the signal in and out from the microcontroller. This port is used to route the analog signal which is to be digitized and to the ADC_12 module of the microcontroller. ‘LCD display’ module is used to display the Bluetooth and board parameters that are configured using the microcontroller. “Switch” is used to select or navigate through the Bluetooth operators on the LCD screen.

‘RF1’, ‘RF2’ and ‘RF3’ headers are the ports to which few pins of the MSP430BT5190 are connected. “R” is the reset button for the experimenter board. The

RF1 and RF2 connectors are connected to few ports of the MSP430BT5190 microcontroller. RF3 connector is used to route some of the missed pins from MSP430BT5190 to the RF1 and RF2 connectors. An RF3 adapter board is used to make these routing connections on the experimenter board.



Figure 4.14. PAN1323 Evolution Module Kit for Bluetooth Operation

In figure 4.14, PAN1323 is the integrated chip from Panasonic Inc. which incorporates the CC2560 Bluetooth core technology from Texas Instruments Inc. At the back of this board there will be two jumper sockets that can be exactly fixed onto the RF1 and RF2 headers on the MSP-EXP430F5438 experimenter board to facilitate the serial communication for instructions and data transfer between the two boards. The interconnection between the two boards is shown in figure 4.15 where the female jumpers on PAN1323 board sits into the male headers on MSP-EXP430F5438 Board.

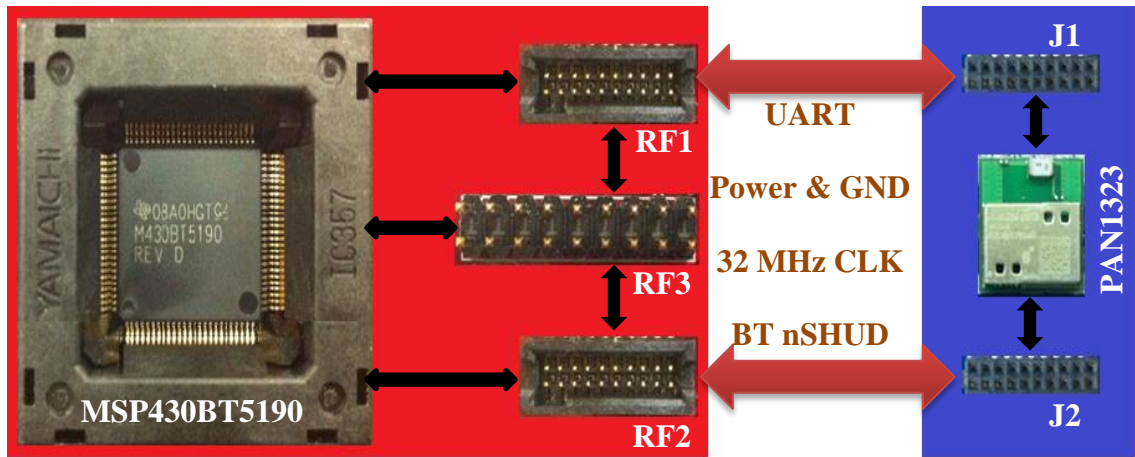


Figure 4.15 Hardware Interconnections between MSP-EXP430F5438 and PAN1323EMK

4.3.2. Software Development

After the necessary hardware connections are made, software has to be developed to run on the microcontroller which can digitize the data and control the Bluetooth operation on the PAN1323 controller. EtherMind Bluetooth software development kit (EMBSDK) for MSP430BT5190-CC2560 platform is used to develop the software on IAR Embedded workbench Integrated Development Environment (IDE) software which is also used to download the program onto the MSP430BT5190 via MSP-FET430UIF USB debugging interface connected to the computer. The PAN1323 controller runs on the FreeRTOS operating system. The Bluetooth related Application Programmers Interfaces (APIs) which implements the Bluetooth Serial Port Profile are provided as a source file in the EMBSDK. The EMBSDK also provides all the source and header files needed for the microcontroller to initialize and operate all the hardware components and connections on the MSP-EXP430F5438 experimenter board including the liquid crystal display.

4.3.2.1. Analog to Digital Conversion

The analog input signal is converted into digital signal by the ADC_12 module of the microcontroller. The registers of the ADC_12 module are configured with the values shown in the table 4.3 to perform the analog to digital conversion. The analog signal is connected to the 13th analog channel (out of 16 total analog input channels) of the ADC_12 module to convert with the 4.8 KHz sampling rate at 12-bit resolution. The reference voltage boundaries for the ADC conversion are GROUND and internal 2.5V from ADC_12 module reference generator i.e. the voltage of the input analog signal should be in the range of 0 V to 2.5 V for the accurate conversion. The result of this conversion is stored in the ADC12MEM0 register. Table 4.3 shows the configurations of the ADC_12 registers.

Table 4.3. ADC_12 Register Initialization for 12-bit Analog to Digital Conversion

Register	Value	Significance
ADC12CTL0	0x0FE3	Enable ADC_12 Module, 1024 adc_clk cycles for sampling period, continuous conversion, 2.5V Internal Reference, Start Conversion bit (ADC12SC).
ADC12CTL1	0x0206	ADC12OSC (5 MHz) clock (adc_clk) source, SAH source (ADC12SC), Repeat ADC conversion.
ADC12CTL2	0x0050	Temperature Sensor OFF, 12-bit Resolution (ADC12RES)
ADC12MCTL0	0x001D	Reference Selection (ADC12REF), Input Analog Channel (ADC12INCH)

$$\text{Sampling Rate} = \frac{1}{\text{Sample time} + \text{Hold time}} = \frac{1}{1024 \text{ clks} + 13 \text{ clks}} = \frac{1}{1037 \times \frac{1}{5 \text{ MHz}}} = 4.82 \text{ KHz}$$

The ADC conversion in the microcontroller is an interrupt driven i.e. an interrupt is generated after each conversion to store the converted data into the specified register. The implementation of the ADC conversion is carried out by connecting the known signals to the analog input port. The converted result in the ADC_12 is converted into integer value and displayed on the LCD which is shown in the figures 4.16 and 4.17.

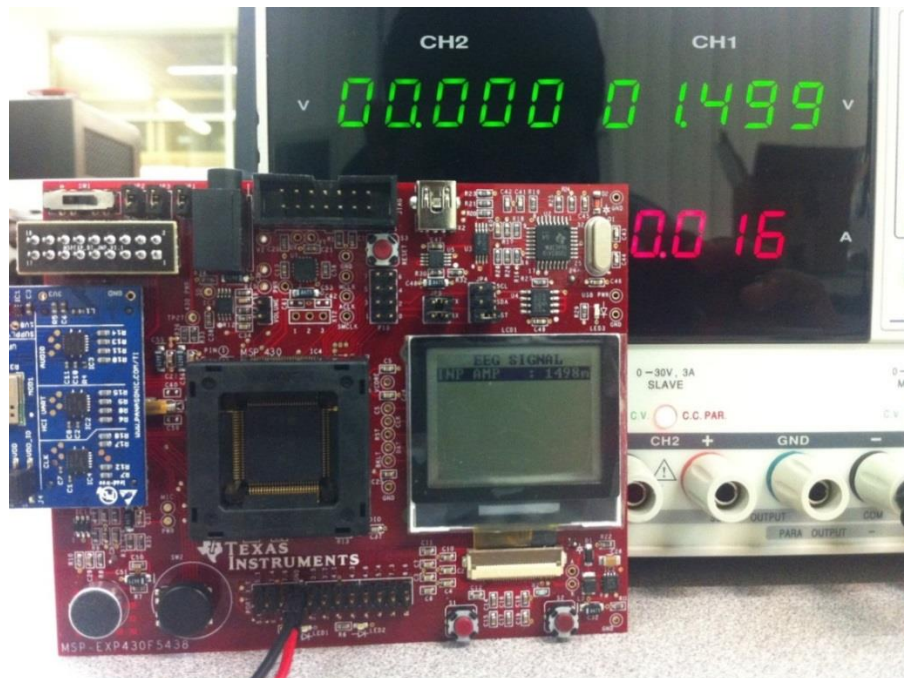


Figure 4.16. ADC Conversion Result Shown on LCD for 1.5 V DC Signal

The 12-bit ADC conversion is implemented and tested for its reliability by varying the known voltage from lower reference voltage to the upper reference voltage i.e. 0V to 2.5V. From this implementation, the ADC conversion is observed to be very precise and accurate enough to use in this design even at the threshold limits.

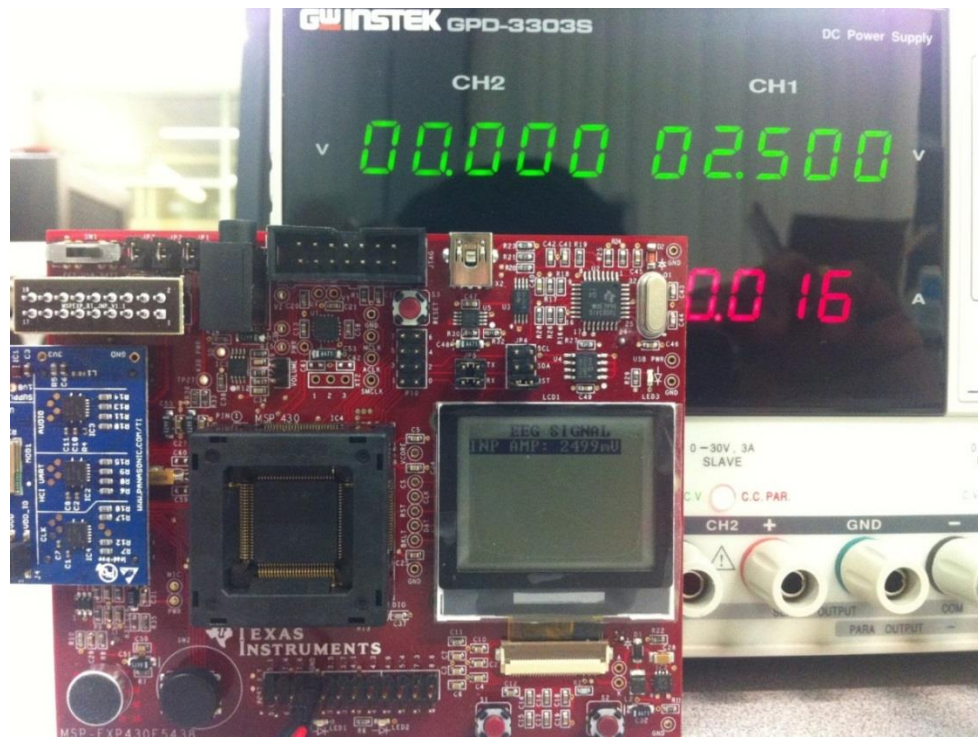


Figure 4.17. ADC Conversion Result Shown on LCD for 2.5 V DC Signal

4.3.2.2. UART Interface (Universal Serial Communication)

The data between the MSP430BT5190 microcontroller and the PAN1323 Bluetooth controller is transmitted from the Universal Serial Communication Interface module of the microcontroller in UART mode. The UART transmission is administered by the registers in the USCI_B module of the microcontroller. The baud rate selected for this data transmission is 115200. Table 4.4 shows the registers and its values, port assignments configured for the UART data transmission as defined in the UART section of the chapter III.

Table 4.4. USCI Register and Port Initialization for UART Transmission

Register / Port	Value / Pin	Significance
UART TxD	P 9.4	Transmit serial data bit stream
UART RxD	P 9.5	Receive serial data bit stream
UART CTS	P 1.3	Clear to send control signal
UART RTS	P 1.4	Request to send control signal
UCA2CTL0	0x00	No Parity, 8-bit data, 1 stop bit, asynchronous UART Transmission
UCA2CTL1	0x80	SMCLK (32 KHz) as USCI clock source.
UCA2MCTL	0x04	Baud Rate generation pattern
UCA2BR0	0x00	Baud Rate (115200)
UCA2BR1	0x9C	Baud Rate (115200)

The baud rate configured for this UART transmission is displayed on the LCD screen along with the other board parameters which give information about the version of the software, type of microcontroller, voltage and frequency of the board and is shown in the figure 4.18.

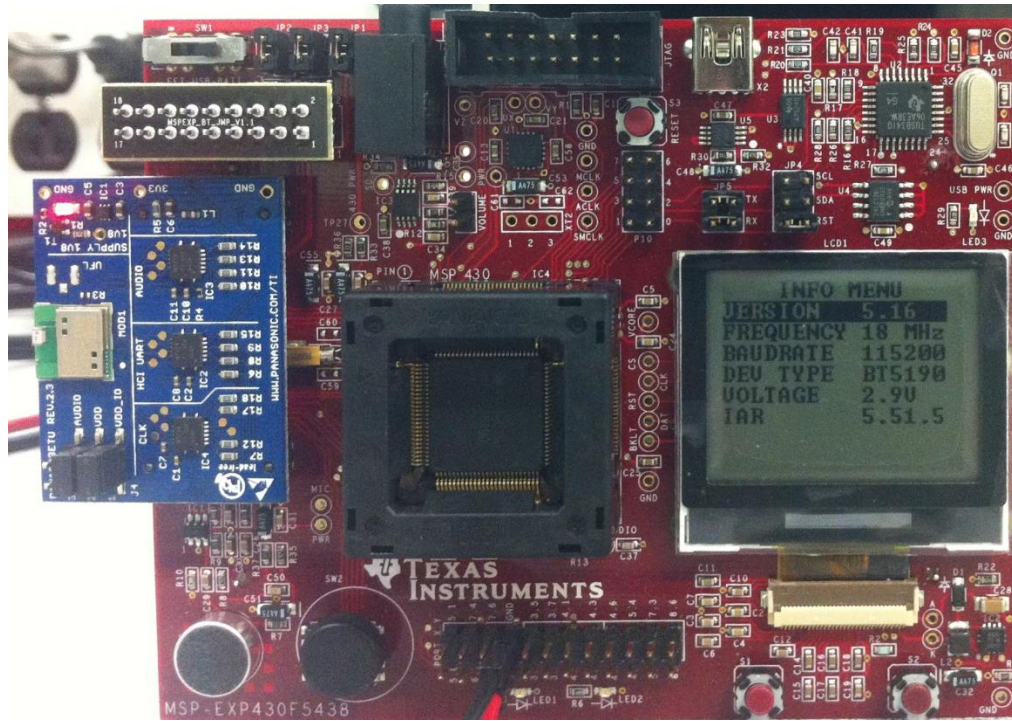


Figure 4.18. Configuration of Experimenter Board

From figure 4.18, ‘VERSION’ is the software version of the EtherMind Bluetooth SDK, ‘FREQUENCY’ is the frequency of the SMCLK signal, ‘BAUDRATE’ is the baud rate at which the data transfers via UART interface, ‘DEV TYPE’ is the type of microcontroller used on the experimenter board, ‘VOLTAGE’ is the power supply to the board, ‘IAR’ is the software version of the IAR Embedded Workbench which is used to develop the software for this Bluetooth operation.

4.3.2.3. Bluetooth Operation

The Bluetooth stack operation is carried out by the FreeRTOS configured on the PAN1323 controller by the Bluetooth specific Application Programmers Interface functions which are collectively defined as the Bluetooth Serial Port Profile (SPP). The Bluetooth SPP defines Bluetooth stack layer protocols [27] which connects and transmits

the data to other devices via serial communication. The appropriate controls and the ADC converted data is given to the APIs handling the Bluetooth connectivity and transfer. The sequential implementation of the Bluetooth operation to search and connect to a device and send the data to the connected device is shown in the figures 4.19 to 4.23 in sequential operations. The ‘Switch’ navigator button described in the hardware section is used to select and navigate through the Bluetooth Menu.

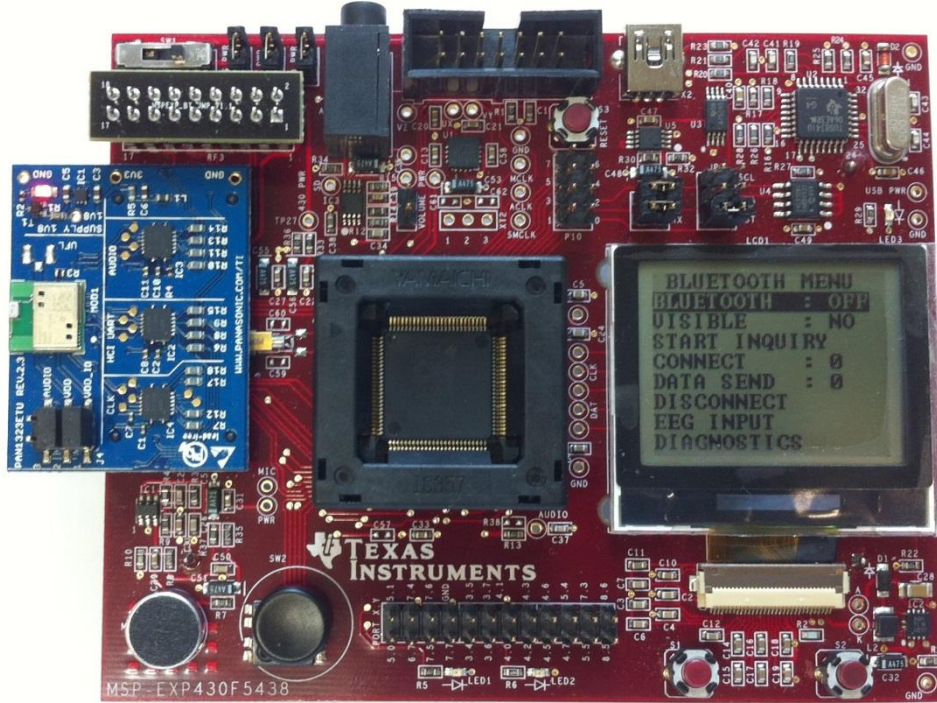


Figure 4.19. LCD Indication of Bluetooth Menu on Board Startup

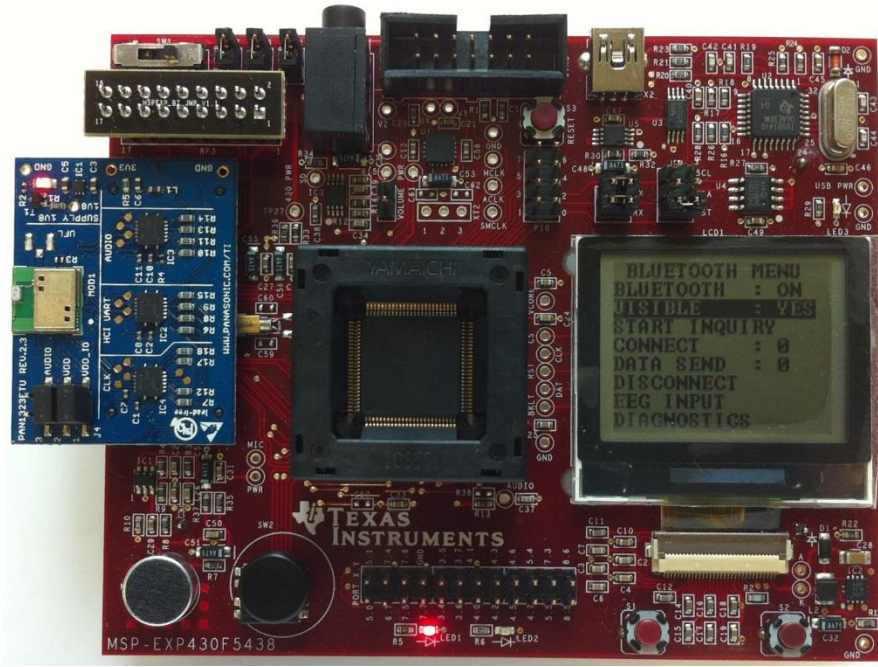


Figure 4.20. LCD Indication of Turning ON Bluetooth & Device Visibility

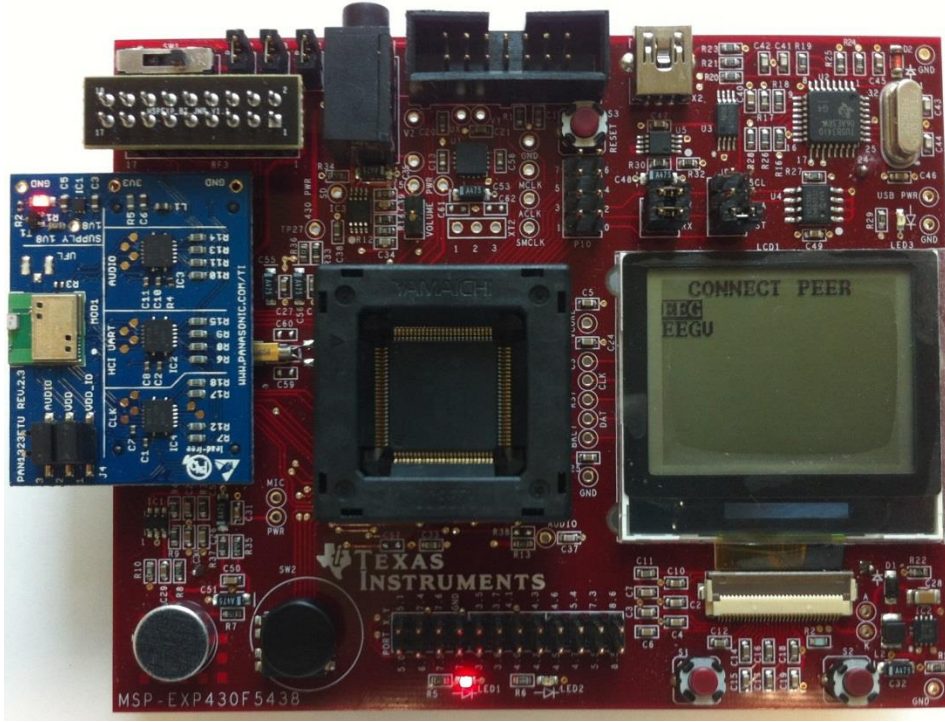


Figure 4.21. LCD Indication of Bluetooth Devices with SPP upon Discovery

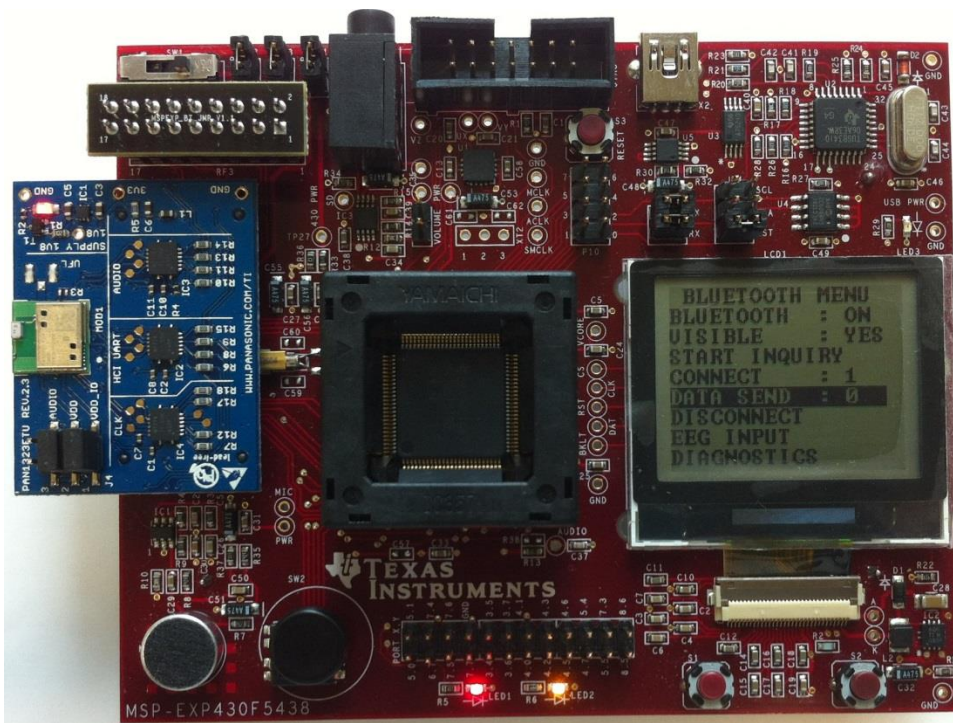


Figure 4.22. LCD Indication of Successful Device Connection

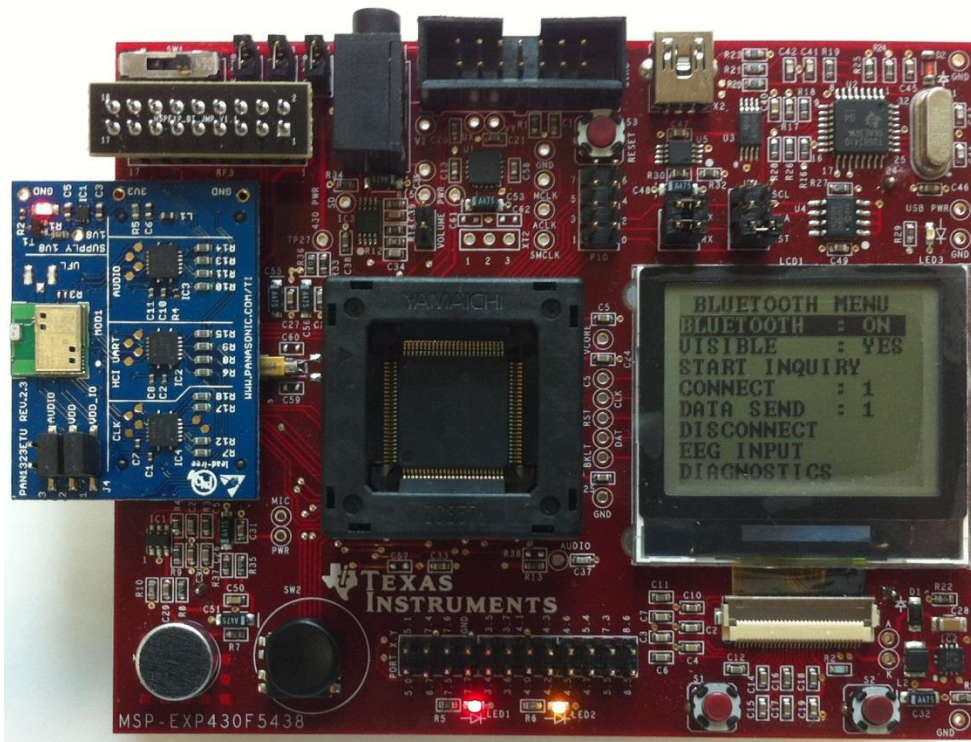


Figure 4.23. LCD Indication of Data Transfer to Connected Device

As shown in figures 4.19 to 4.23, after turning on the Bluetooth and its visibility of the board, the device search is performed and devices which support Serial Port Profile are shown. Once the successful connection is established, data transfer is initiated. Apart from LCD Indication, the Red LED on bottom indicates that the Bluetooth on PAN1323 is switched on. The Orange LED indicates that the PAN1323 is connected to a device and if it blinks, it indicates that the data is being transmitted to the connected device.

4.4. Android Software Implementation

The software application that will be installed on the Android operated mobile phone is developed which implements the algorithm designed in the chapter III. This application is developed using the Android software development kit provided by the Android developer's website.

The application titled as “EEGscope” is installed on the mobile device which operates on Android system. The functionality of the application is tested with a sinusoidal input from the analog front end used in the previous testing to the experimenter board. The Graphical User Interface of the ‘EEGscope’ Application with no activity after start up is shown in figure 4.24.



Figure 4.24. Graphical User Interface of ‘EEGscope’ App on Android

During the initialization of Graphical User Interface (GUI), the application checks for the Bluetooth compatibility of the device. As shown in figure 4.24, there will be two buttons on the GUI, one on the bottom of the GUI is to search and connect to a device and the other one on the top (run) is to acquire data from the connected device.

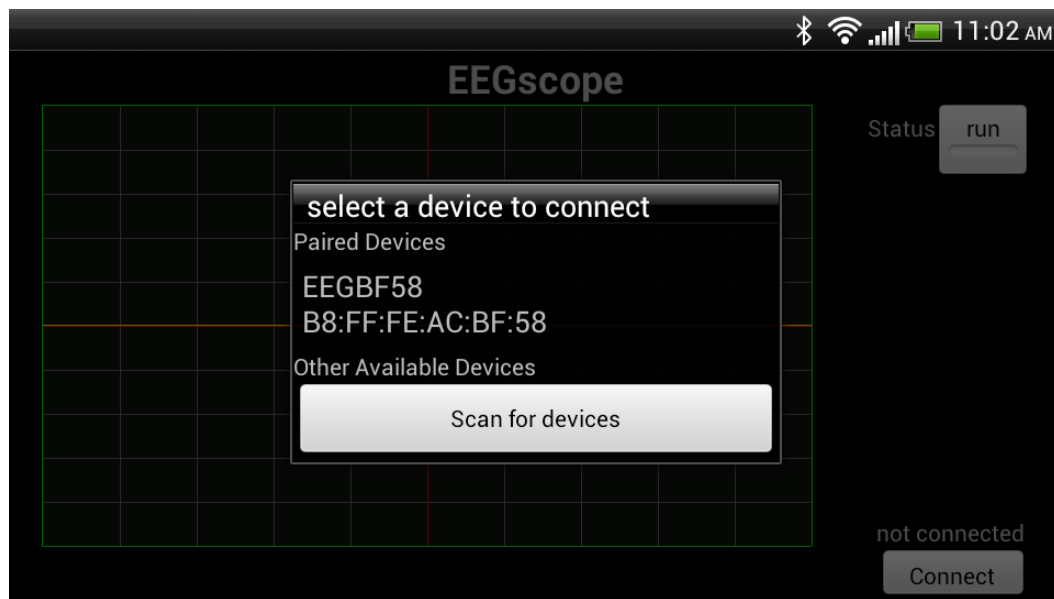


Figure 4.25. Screenshot of ‘EEGscope’ Scan for Available Devices.

When the bottom button is pressed, the application scans for the available Bluetooth devices and display the pop up list as shown in figure 4.25. ‘EEGBF58’ is the name configured for PAN1323 Bluetooth chip. From the list of available devices, one has to tap on the required device to make a connection. The GUI indicates the status of the connection as shown in figure 4.26 just above the connect button.



Figure 4.26. Screenshot of ‘EEGscope’ Connection Status with ‘EEGBF58’

After the successful connection is made with PAN1323 device, the ‘run’ button on the top is tapped to start receiving the data and display on the real time plot. This is shown in figure 4.27.



Figure 4.27. Real Time Plotting of Received Data per 1 Second Interval on ‘EEGscope’

The data reception on the ‘EEGscope’ application is not consistent as observed from the plot on GUI in figure 4.26. This is occurred due to the non-uniform data flow by the Bluetooth serial port profile stack implemented by the PAN1323 unit. The ADC result is accessed once it transmits the current value and ADC is not functioned while transmission. The android application receives approximately 750 samples of signal data per 1 second which is displayed on the user interface after successive accumulations for 1 second time intervals. To implement the continuous transmission, more expertise in Bluetooth stack design is needed along with a new host controller interface.

4.5. Implementation of Designed EEG Acquisition System

The EEG acquisition system is developed by cascading the analog and digital front end designs after validating these designs separately using the sample signals as described in the above sections. The designed prototype is implemented to collect the EEG signals from the recruited subject following the guidelines from Human Subject

Institutional Review Board (HSIRB) with approval shown in Appendix. The setup for acquiring the EEG signals from the subject is shown in figure 4.28.

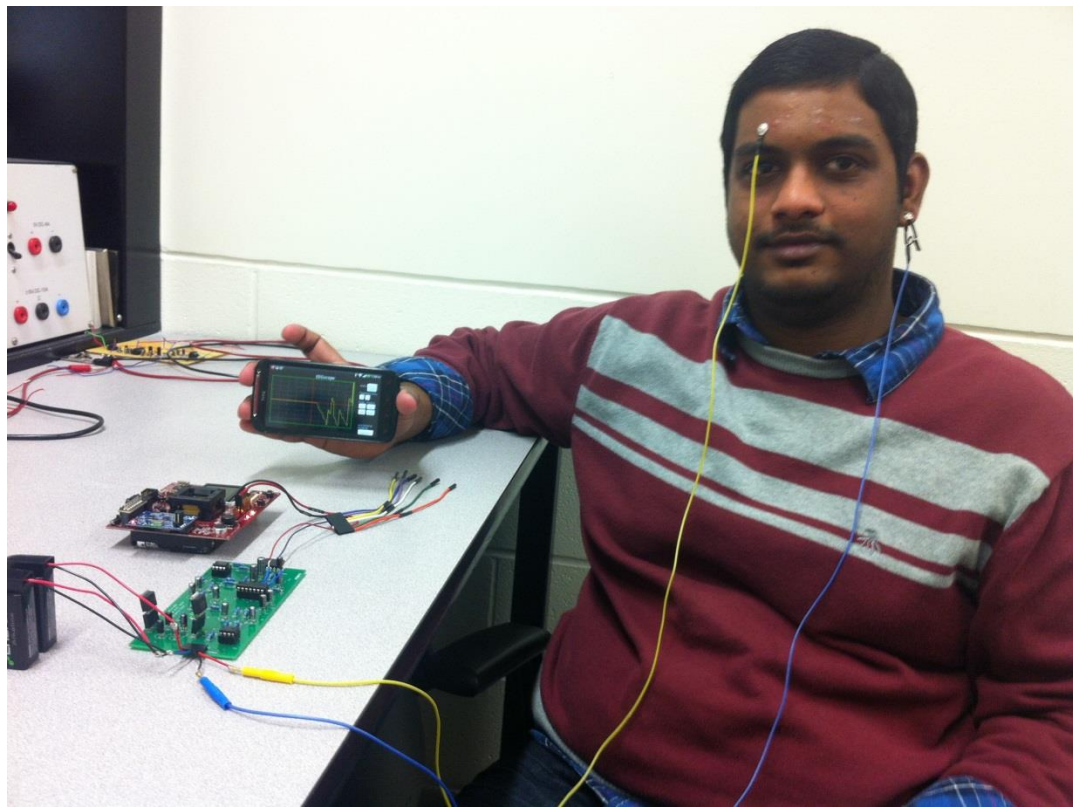


Figure 4.28. Setup of Designed Prototype for EEG Acquisition System used on a Subject

As shown in figure 4.28, the analog circuitry is powered using the two 9V batteries and the digital circuit is powered using two AA batteries of 3V each. The electrodes are attached to the forehead region of the subject to collect the EEG signals and are connected to the amplifier input channels of the analog circuitry on the other end. The output of the analog circuitry is connected to the analog input pin of the MSP430BT5190 microcontroller on the digital circuitry. The mobile phone with the developed android application installed on it is connected to the Bluetooth controller on the digital board. After successful connection the designed prototype transmits the signal

to the android application. The reception and plotting of the EEG signals on the “EEGscope” application user interface is shown in the figure 4.29.

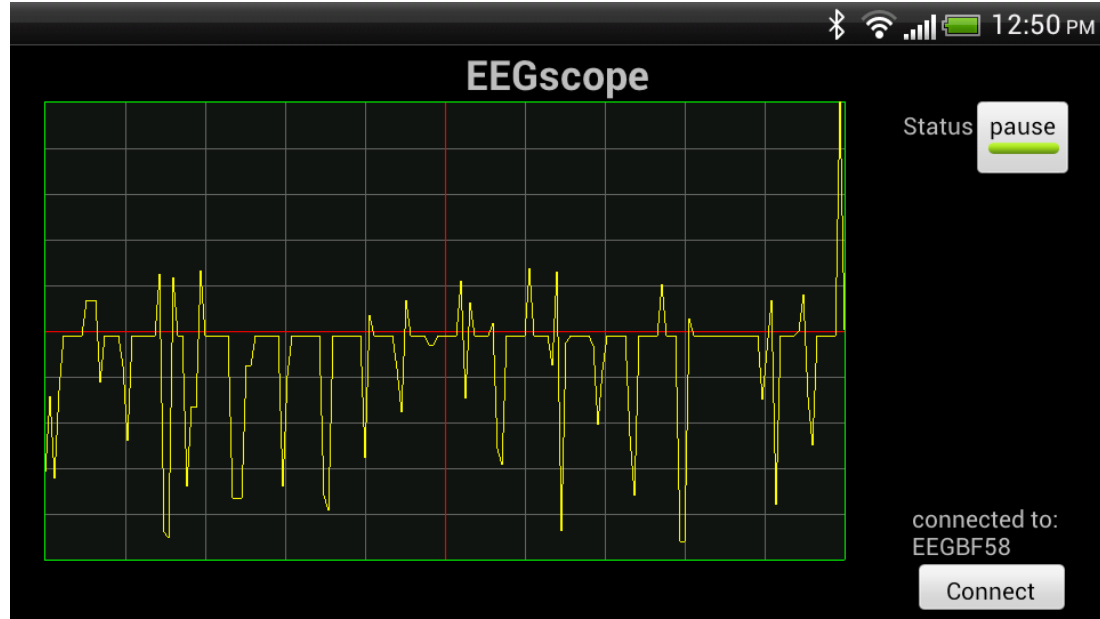


Figure 4.29. Display of Received EEG Signals on the ‘EEGscope’ Android App

4.6. Summary

The designed prototype system in the chapter III is implemented and analyzed at different stages. The analog circuitry is realized on the printed circuit board and tested with the sample signals to obtain the frequency response and gain of the analog circuitry. The digital data transfer is realized using the MSP430BT5190 microcontroller and PAN1323 Bluetooth controller to digitize and transfer the signal collected from the analog circuitry to the Android operated mobile using Bluetooth communication. This design is validated by collecting the signals from the subject and transmitting to the Android mobile after preconditioning.

CHAPTER – V

CONCLUSIONS AND FUTURE SCOPE

5.1. Conclusions

In this thesis, I present the design and implementation of prototype hardware for acquiring the Electroencephalographic signals from the human subject and display them on the android mobile. The EEG signals acquired from the subject were pre-conditioned to be amplified with a 73.84dB gain which is ideally designed for 74dB gain. The corner frequencies for the filter stage are 0.5Hz, 59Hz, 65Hz and 87Hz i.e. the filter attenuates the frequencies less than 0.5Hz, in between 59Hz to 65Hz and more than 87Hz in this implementation which is ideally designed to pass the frequencies between 0.5Hz to 100Hz rejecting 60Hz. The gain of the pass band frequencies is between 0dB and -3dB which is designed for 0dB gain. These shifts in the gain and corner frequencies is due to the change in the analog component values due to their tolerance and also due to the unavailability of appropriate spectrum analyzer, which was a challenge through the project, to appropriately measure the frequency response.

The EEG signal received from the analog end is digitized and transmitted to the Bluetooth controller (PAN1323) by the MSP430BT5190 microcontroller. The analog signal is digitized with 12 bit resolution between the voltage ranges of 0V and 2.5V references voltages. The signal is transmitted via serial communications interface in UART mode with 115200 baud rate. The microcontroller is the host controller for the Bluetooth serial port profile implemented by the PAN1323 module. “EEGscope” Android application is developed and installed on the mobile and connected to the

Bluetooth controller. The android application receives the data and displays it on the user interface of the application, awaiting for further actions, such as analysis and alert signal.

After successful Bluetooth connection, the ‘EEGscope’ application displays the data after accumulating 750 samples of incoming signal data per one second time interval. The authenticity of the data further has to be analyzed.

5.2. Recommendations for Future Work

In this project, we faced several challenges and have several suggestions to expand and/or enhance the design and the results, these include:

1. Examination of noise and time delay during the signal transmission in the analog circuit and during Bluetooth transmission need to be investigated.
2. The digital circuit and its software have to be optimized for the signal transmission via Bluetooth, i.e. reduction in the microcontroller usage for other board’s related functionalities by designing a new circuit to interface microcontroller with the Bluetooth chip intended for ADC conversion and UART operation.
3. The user interface of the Android application has to be optimized to receive and update the waveform in real time along with the accumulation of data for further analysis.
4. The discrepancies in the analog implementation can be avoided by implementing the filtering processes digitally using appropriate microcontroller.

APPENDIX

HSIRB Approval Letter (Proj. No.: 11-11-12)

WESTERN MICHIGAN UNIVERSITY



Human Subjects Institutional Review Board

Date: December 13, 2011

To: Ikhlas Abdel-Qader, Principal Investigator
Veerendra Dasari, Student Investigator for thesis
David Anderson, Student Investigator
Abdoulaye Ousseini, Student Investigator
Angie Massiel Paula Sanchez, Student Investigator

From: Victoria Janson, Interim Chair

A handwritten signature of Victoria Janson.

Re: HSIRB Project Number 11-12-12

This letter will serve as confirmation that your research project titled “EEG Signal Acquisition System” has been **approved** under the **expedited** category of review by the Human Subjects Institutional Review Board. The conditions and duration of this approval are specified in the Policies of Western Michigan University. You may now begin to implement the research as described in the application.

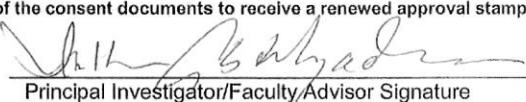
Please note that you may **only** conduct this research exactly in the form it was approved. You must seek specific board approval for any changes in this project. You must also seek reapproval if the project extends beyond the termination date noted below. In addition, if there are any unanticipated adverse reactions or unanticipated events associated with the conduct of this research, you should immediately suspend the project and contact the Chair of the HSIRB for consultation.

The Board wishes you success in the pursuit of your research goals.

Approval Termination: December 13, 2012

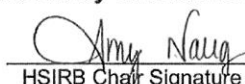
HSIRB Project Number: 11-12-12

5. Have there been changes in Principal or Co-Principal Investigators? Yes No
(If yes, provide details on an "Additional Investigators" form (available at the HSIRB web site, http://www.wmich.edu/research/compliance/hsirb/hsirb_2.html.)
6. Has the approved protocol been modified or added to with respect to:
(If yes to any item below, provide the details on an attached sheet.)
- | | | |
|--------------------|------------------------------|--|
| a. Procedures | <input type="checkbox"/> Yes | <input checked="" type="checkbox"/> No |
| b. Subjects | <input type="checkbox"/> Yes | <input checked="" type="checkbox"/> No |
| c. Design | <input type="checkbox"/> Yes | <input checked="" type="checkbox"/> No |
| d. Data collection | <input type="checkbox"/> Yes | <input checked="" type="checkbox"/> No |
7. Has any instrumentation been modified or added to the protocol? Yes No
(If yes, attach new instrumentation or indicate the modifications made.)
8. Have there been any adverse events that need to be reported to the HSIRB? Yes No
(If yes, provide details on an attached sheet.)
9. Total number of subjects approved in original protocol: 00005
10. Total number of subjects enrolled so far: 2
If applicable: Number of subjects in experimental group: _____ Number in control group: _____
• If this is a FINAL REPORT you may stop here and return the form electronically.
• If this is an APPLICATION FOR CONTINUING REVIEW continue with numbers 11-13 below.
11. Estimated number of subjects yet to be enrolled: 0
12. Verification of Consent Procedure: Provide copies of the consent documents signed by the last two subjects enrolled in the project. Cover the signature in such a way that the name is not clear but there is evidence of signature. If subjects are not required to sign the consent document, provide a copy of the most current consent document being used.
13. If you are continuing to recruit subjects for this project, please remember to include a clean original of the consent documents to receive a renewed approval stamp.

 10/4/12
Principal Investigator/Faculty Advisor Signature Date

 10/03/2012
Co-Principal or Student Investigator Signature Date

Approved by the HSIRB:

 11/13/12
HSIRB Chair Signature Date

Western Michigan University
Human Subject Institutional Review Board – Mail Stop 5456
(269) 387-8293 research-compliance@wmich.edu

Revised 7/03 WMU HSIRB
All other copies obsolete.

BIBLIOGRAPHY

- [1] John G Webster, *Medical Instrumentation: Application and Design*, 3rd ed., New York: John Wiley & Sons Inc., 1998.
- [2] Richard Aston, *Principles of Biomedical Instrumentation and Measurement*, New York: Macmillan Publishing Company, 1990.
- [3] Saeid Sanei and J. A. Chambers, *EEG Signal Processing*, New Jersey: John Wiley & Sons Inc., 2007.
- [4] Xun Chen; Wang, J., "Design and Implementation of a Wearable, Wireless EEG Recording System," *Bioinformatics and Biomedical Engineering, (iCBBE) 2011 5th International Conference on* , vol., no., pp.1,4, 10-12 May 2011.
- [5] Drakulic, B.S.; Berry, S.J.; Sterman, M.B., "A portable EEG recording system," *Engineering in Medicine and Biology Society, 1989. Images of the Twenty-First Century., Proceedings of the Annual International Conference of the IEEE Engineering in* , vol., no., pp.1395,1396 vol.5, 9-12 Nov 1989.
- [6] Filipe, S.; Charvet, G.; Foerster, M.; Porcherot, J.; Beche, J.F.; Bonnet, S.; Audebert, P.; Regis, G.; Zongo, B.; Robinet, S.; Condemeine, C.; Mestais, C.; Guillemaud, R., "A wireless multichannel EEG recording platform," *Engineering in Medicine and Biology Society,EMBC, 2011 Annual International Conference of the IEEE* , vol., no., pp.6319,6322, Aug. 30 2011-Sept. 3 2011.
- [7] Saadi, H.; Ferroukhi, M.; Attari, M., "Development of wireless high immunity EEG recording system," *Electronic Devices, Systems and Applications (ICEDSA), 2011 International Conference on* , vol., no., pp.120,124, 25-27 April 2011.
- [8] Whitchurch, A.K.; Abraham, J.K.; Lonkar, M.A.; Varadan, Vijay K., "Design of a Compact Amplifier and Signal Conditioning Module for Wireless EEG Monitoring," *Region 5 Technical Conference, 2007 IEEE* , vol., no., pp.153,156, 20-22 April 2007.
- [9] Tompkins, Willis J., "Evolution of microcomputer-based medical instrumentation," *Engineering in Medicine and Biology Society, 2009. EMBC 2009. Annual International Conference of the IEEE* , vol., no., pp.6590,6593, 3-6 Sept. 2009.
- [10] Sergio Franco, *Design with Operational Amplifiers and Analog Integrated Circuits*, 3rd ed., New Delhi: Tata McGraw-Hill, 2002.
- [11] Chiu-Chiao Chung; Ching Yuan Huang; Shiau-Chin Wang; Cheng-Min Lin, "Bluetooth-Based Android Interactive Applications for Smart Living," *Innovations in Bio-inspired Computing and Applications (IBICA), 2011 Second International Conference on* , vol., no., pp.309,312, 16-18 Dec. 2011.

- [12] Junwei Duan; Changhao Chen; Sio Hang Pun; Feng Wan; Peng Un Mak; Pui In Mak; Mang I Vai; Yong Hu, "A Wearable Wireless General Purpose Bio-signal Acquisition Prototype System for Home Healthcare," *Biomedical Engineering and Biotechnology (iCBEB), 2012 International Conference on* , vol., no., pp.1176,1179, 28-30 May 2012.
- [13] Texas Instruments, "INA128 Precision, Low Power Instrumentation Amplifier," <http://www.ti.com/lit/ds/symlink/ina128.pdf>, [January 21, 2012].
- [14] Texas Instruments, "TLV2264 Advanced LinCMOS (TM) Rail-to-Rail Operational Amplifier," <http://www.ti.com/lit/ds/symlink/tlv2264.pdf>, [January 21, 2012].
- [15] STMicroelectronics, "LM258 Low power Dual Operational Amplifier," http://www.st.com/internet/com/TECHNICAL_RESOURCES/TECHNICAL_LITERATURE/DATASHEET/CD00000464.pdf, [September 29, 2012].
- [16] Texas Instruments, "Op-amps for Everyone Design Guide," Rev. B, <http://www.ti.com/lit/an/slod006b/slod006b.pdf>, [January 09, 2012].
- [17] Texas Instruments, "UA7805 5V Fixed Positive Voltage Regulator," <http://www.ti.com/lit/ds/symlink/ua7805.pdf>, [December 16, 2012].
- [18] Texas Instruments, "UA7905 5V Fixed Negative Voltage Regulator," <http://www.ti.com/lit/ds/symlink/ua7905.pdf>, [December 16, 2012].
- [19] Texas Instruments, "MSP430BT5190 Mixed Signal Microcontroller," <http://www.ti.com/lit/ds/symlink/msp430bt5190.pdf>, [March 10, 2012].
- [20] Texas Instruments, "PAN1323 Evolution Module Kit," <http://www.ti.com/tool/pan1323emk>, [March 10, 2012].
- [21] Texas Instruments, "MSP-EXP430F5438 Experimenter Board," <http://www.ti.com/lit/ug/slau263g/slau263g.pdf>, [March 10, 2012].
- [22] Texas Instruments, "MSP-FET430UIF USB Debugging Interface," <http://www.ti.com/lit/ug/slau278l/slau278l.pdf>, [March 10, 2012].
- [23] Texas Instruments, "MSP430X5XXX User guide," <http://www.ti.com/lit/ug/slau208l/slau208k.pdf>, [March 10, 2012].
- [24] "Bluetooth Oscilloscope," <http://projectproto.blogspot.com/2010/09/android-bluetooth-oscilloscope.html>, [December 16, 2012].
- [25] "Android Developers," <http://developer.android.com/training/index.html>, [December 16, 2012].

[26] Nassir, A.; Barnea, O., "Wireless body-area network for detection of sleep disorders," *Electrical & Electronics Engineers in Israel (IEEEEI), 2012 IEEE 27th Convention of*, vol., no., pp.1,5, 14-17 Nov. 2012.

[27] Texas Instruments, “MSP430BT5190+cc2560 EtherMind Bluetooth SDK Developer’s Guide,” <http://www.ti.com/tool/mt-bt-sdk>, [March 10, 2012].